

CTA-GPS

November 11, 2020

1 Analysis strategy and definitions

The code of the catalogue production prototype described in the following is available on GitHub (limited access):

<https://github.com/gammasky/cta-2020-gps-analysis>

1.1 Datasets

We study the Galactic Plane within $-180 < l < 180$ and $|b| < 6$. We consider all simulated observations in this range. The data are divided in two datasets with different energy ranges $E = 0.07\text{-}1$ TeV (subTeV) and $E = 1\text{-}200$ (postTeV). This separation is meant to improve the object detections as different populations of sources have different optimal detection range. This separation is also useful to improve fitting performance saving time and memory. Indeed as the PSF-resolution is coarser at low energy the subTeV dataset can be defined with a coarser binning. The subTeV and postTeV datasets are defined with a spatial binning of 0.06 and 0.03 degree, respectively. For each dataset the energy axis contains 10 bins per decade. We impose a smaller offset cut at low energy as the instrument background is larger. So the subTeV and postTeV datasets include the observations with a 3 and 5 degree off-set cut, respectively.

Note that in a first time the catalogue production assumes the exact simulated model for instrumental and diffuse backgrounds. In a second time we will consider alternative or biased backgrounds in a separate test branch in order to study the impact of backgrounds modeling uncertainties on the catalogue production.

1.2 Object detection

The goal is to build in a short amount of computational time a list of potentially valuable objects without prior case-specific morphological assumptions. This list provides source candidates, with robust guess on their position and morphological parameters, to be tested by conventional analyses using template-fitting.

The first step is to compute the significance of the excesses above a given background model (instrumental+diffuse). The significance maps are produced for different correlation radius, $R_{corr} = 0.06, 0.1, 0.2$ degree and for the two energy ranges considered $E=0.07\text{-}1\text{-}200$ TeV. The significance maps are filtered by hysteresis thresholding with a high threshold of 4σ and a low threshold of 2σ (pixels between these two thresholds are preserved only if they are continuously connected to a pixel above the high threshold). Then the object detection combines three methods:

- Peak detection: local maximum in the hysteresis-filtered significance maps

- Blob detection: groups of pixel isolated by the hysteresis filtering are modeled as circle if its filling factor larger is than 80 %
- Edge detection and Hough circle detection (for details see arxiv.org/abs/2005.05176)

Peak detection is performed on significance maps with $R_{corr} = 0.06, 0.1, 0.2$ degree for each of the two energy ranges. The blob and Hough detection are performed only for $R_{corr} = 0.1$ deg in the 1-200 TeV energy range in order to take advantage of the finest PSF-resolution.

1.3 Associateons

In order to associate the detected objects with the known sources we test for spatial coincidence using two criteria based on inter-center distance and surface overlap. For each object we search for known sources within an inter-distance:

$$d_c < 0.1 + 0.3 \times R_{object} \quad (1)$$

and we report only the source maximizing the surface overlap fraction, defined as:

$$SF_{overlap} = \frac{S_{object} \cap S_{source}}{S_{object} \cup S_{source}}. \quad (2)$$

We choose to report only the strongest coincidence in order to limit the possible associations for extended objects. We also enforce that each source can be associated to only one object and conversely.

For detected objects the surface is computed as a disk of radius R_{object} , while for the fitted and simulated sources we consider the surface delimited by the iso-contours in flux corresponding to a 68% containment.

This association criterion is used to match the detected objects with simulated sources. In order to overhaul the quality of the catalogue production algorithm components we introduce the following diagnostic quantities:

- the reconstruction fraction, $f_{reco} = N_{asso} / N_{source}$, fraction of simulated sources associated to a detected object referred as the reconstruction fraction
- the association fraction, $f_{asso} = N_{asso} / N_{object}$, the fraction of objects associated to a known source, referred as the association fraction.
- the dissimilarity score defined as $d_{score} = 1 - f_{reco} \times f_{asso}$

In the seeds list files and plots we report all associations with $SF_{overlap} > 0$. but to compute the score quantities we impose a more strict cut at $SF_{overlap} > 0.25$ (limit the association error for more reliable learning-based methods and eventually hyper-parameters optimization).

1.4 Classification and selections

In addition to the association with known sources, we classify and rank the detected objects in order to identify the most promising source candidates and guess their morphology. To do so we rely on a set of morphological parameters:

- the position and radius given by the various detection methods;

- the Pearson correlation coefficient (PCC or Pearson-R) of a 5-point radial profile in flux: for each object we have integrated the flux map (with $R_{corr} = 0.1\text{deg}$) in 5 rings of equal area between the center of the object and its radius;
- a morphology flag, the Pearson-R coefficient of the radial profile in flux is used to distinguish 3 types of structures:
 - Peak $\equiv PCC < -1/3$,
 - Flat $\equiv |PCC| < 1/3$,
 - Cavity $\equiv PCC > 1/3$;
- a nesting flag: for each pair of objects C of radius R and R_{sub} , we calculate their inter-center distance, d , and define 5 overlapping configurations :
 - Class 0 $\equiv C(R) : d > R + R_{sub}, \forall C(R_{sub})$,
 - Class 1 $\equiv C(R) : \exists C(R_{sub}) \mid d \leq R + R_{sub}, R_{sub} \leq R$,
 - Class 2 $\equiv C(R_{sub}) : \exists C(R) \mid d \leq R + R_{sub}, R_{sub} < R$,
 - Class 3 $\equiv C(R_{sub}) : \exists C(R) \mid d \leq R, R_{sub} < R$,
 - Class 4 $\equiv C(R_{sub}) : \exists C(R) \mid d \leq R - R_{sub}, R_{sub} < R$.
- the distance of a sub-structure to its main-object, d_{main}
- the mean distance of the 5 nearest neighbors, d_{5NN}

In the following, Class 0 and 1 are defined as main objects; Class 0 objects are non-overlapping, while Class 1 are large objects partially overlapping with smaller ones. These smaller objects are considered as sub-structures, and are of Class 2, 3 or 4 depending on the inter-center distance to the main object.

For each detected object we compute a test statistic (TS) as the squared significance of the residual excess integrated with a correlation radius equivalent to the object radius. The candidates object are filtered such as $TS_{\{\text{resi}\}} > 10$. Then we perform an outlier detection using the isolation forest algorithm (<https://arxiv.org/pdf/1811.02141.pdf>). The distribution of objects associated to known sources (previously catalogued not the new ones simulated) in the PCC , d_{main} , d_{5NN} parameters space gives us an idea of the expected density of objects and distance between sub-structures depending on shape. These informations are used to rank the candidates objects and reduce the spurious detection of sub-structures in complex sources (that still remain after the deduplication of the very closeby objects).

After the TS filtering and the outlier detection the selected seeds are divided in two lists:

- main: known objects, main objects, sub-structure more significant than their parent with $TS_{\text{diff}} > 25$
- sub: unidentified sub-structures less significant than their parent.

1.5 Model fitting

For the fitting the Galactic plane is divided in 10-degree wide region separated by 5 degree (half-overlapping). A tree degree margin is added to each sub-region to account correctly for the psf

Sub-datasets containing less than five sources are merged with their neighbor in order to limit the number of regions fitted. The 56 sub-regions obtained are then fitted independently.

By default candidates are fitted with a generalized gaussian as spatial model and a [log-parabola](#) as spectral model. The generalized gaussian probability density function is defined as : $f(l, b) \propto \exp(-\left(R(l, b) / R_{\text{eff}}\right)^{(1/\eta)})$. The normalization is computed such as the model integrates to unity. The spatial shape parameter, η , is fitted for values in [0.1, 1]. The spatial model is equivalent to a disk when η tends to zero, a gaussian for $\eta=0.5$ and a Laplacian for $\eta=1$. The minimal size fitted is 0.06 deg (slightly larger than the mean PSF radius at 1 TeV). Alternatively a shell is fitted as spatial model depending on the morphological guess from the detection step (candidates flagged as cavity, or flat with inner sub-structures).

For each sub-regions, the seeds in the main-list are fitted first while the seeds in the sub-list are added only if the remaining residuals excess toward them is still significant $TS_{\text{resi}} > 25$ after the fitting of the main objects. The candidate objects outside the fitting mask but within the dataset margin are merging into an unique background component. So for each energy range we have three backgrounds: instrumental (irf), diffuse (iem), and outer-sources.

The fitting strategies include the following operations:

- fit all main sources radius and spectrum together with backgrounds norm and index (excessively time consuming, disabled in this test branch)
- fit sources by group considering only nested ones (according to NestFlag infos) together with backgrounds (all parameters). Iterate 3 time adding sub-structures progressively depending on their selection score.
- fit only spectral parameters
- test for point source hypothesis against default extended model
- test for additional source (up to 5 per region). Find largest peak above 5σ in significance maps iteratively, added to the final model after the fit only if $TS_{\text{null}} > 25$ in at least one of the energy ranges.
- test for ellipticity (only if the shape of the negative residuals above 1σ has an ellipticity larger than 0.5).
- reduce global model: compute test statistic for the null hypothesis (global model all frozen) and keep only sources with $TS_{\text{null}} > 25$ in at least one of the energy ranges.

Note that the optimal parameters of a model are given by the likelihood maximization, and the selection among alternative models is performed by minimization of the corrected Akaike information criterion (AICc, [burnham and anderson 2002](#)) in order to take into account the difference in number of parameters between models (not necessarily nested).

Once all regions fitting are completed, we assemble the final global model. Models are taken from one dataset only if they are located within 2.5 degrees from the center (because of the overlapping we consider only core regions). Background corrections from each dataset are applied considering the same 2.5 degree window. All quantities and diagnostics shown in the following are computed from this final global model (distributed in yaml and fits formats).

1.6 Models refinement

In order to simplify the global model we search for groups of sources that could be replaced by an alternative model. In particular we scan the source distribution to identify linear, and circular pattern that could be regrouped into single elliptical gaussian, and shell, respectively.

To do so we first extract several complexes by applying two thresholds in the flux map of the fitted model: the first (low) threshold isolates the main complexes and the second (higher) threshold (10% of the complex maximum flux) will separate the bright peaks from the more diffuse regions. Then within each of these blobs we search for sub-groups of sources that best match a linear or circular pattern using **RANSAC algorithm**.

The groups of aligned sources are replaced by an elliptical model if the $\Delta AICc = AICc_{\text{single}} - AICc_{\text{multi}} > 0$ (after fitting). This test results in 13 new ellipticals. Similarly, the circular groups are tested against a shell, but we also consider a shell + gaussian to account for composite sources. This test adds 1 composite. Overall the regrouping procedure removes about 30 objects.

We also look for sources surrounded by positive residuals above 1σ with an ellipticity larger than 0.5, for which we also test an elliptical model. This test results in 1 additional elliptical source.

...

```
[333]: # import
```

```
<IPython.core.display.HTML object>
```

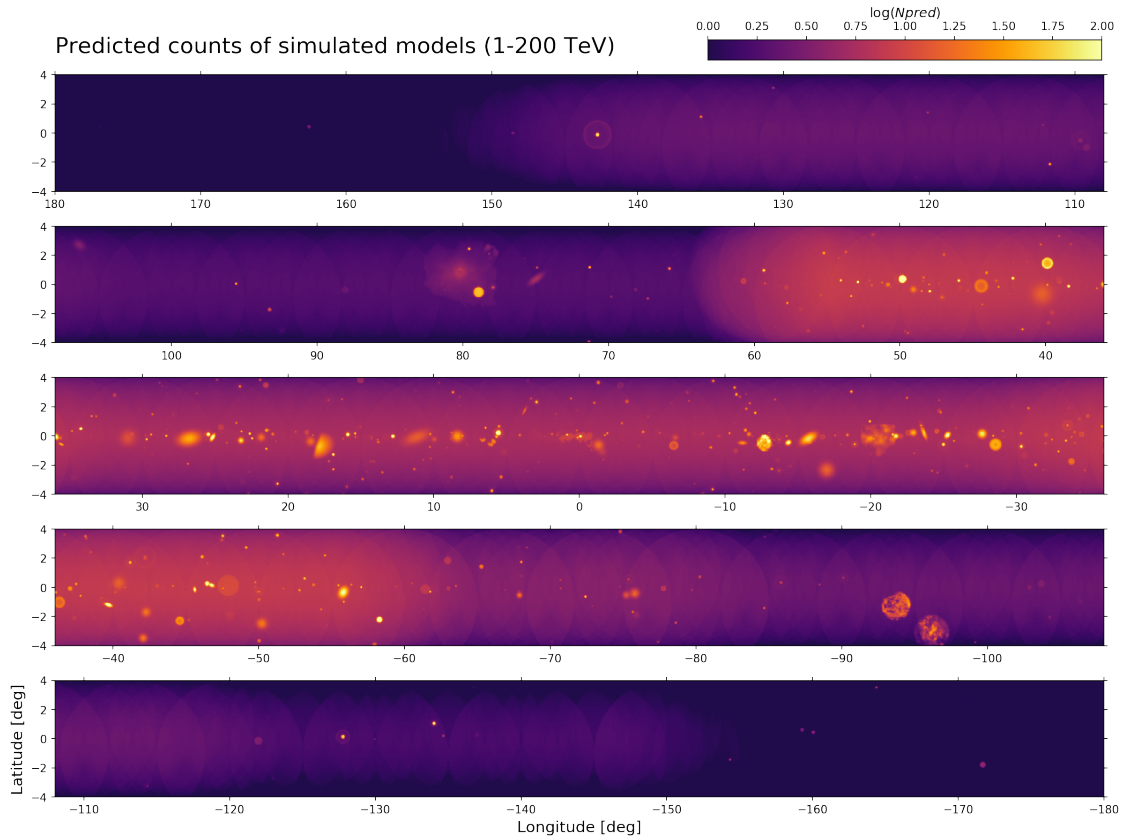
2 Simulated sky

Models files are available on GitHub:

<https://github.com/cta-observatory/cta-gps-simulation-paper/tree/master/skymodel>

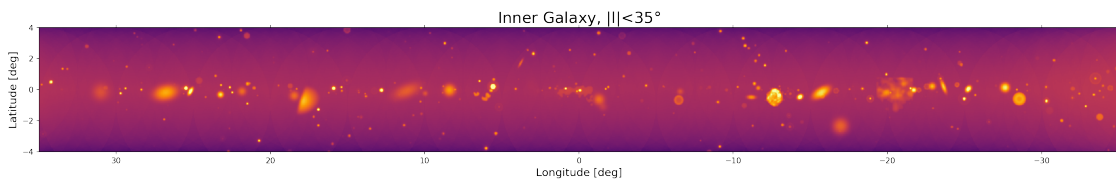
2.1 Predicted counts

```
[334]: # predicted counts (exact models)
```



2.1.1 Zoom toward inner Galaxy

```
[335]: # zoom toward inner Galaxy
```

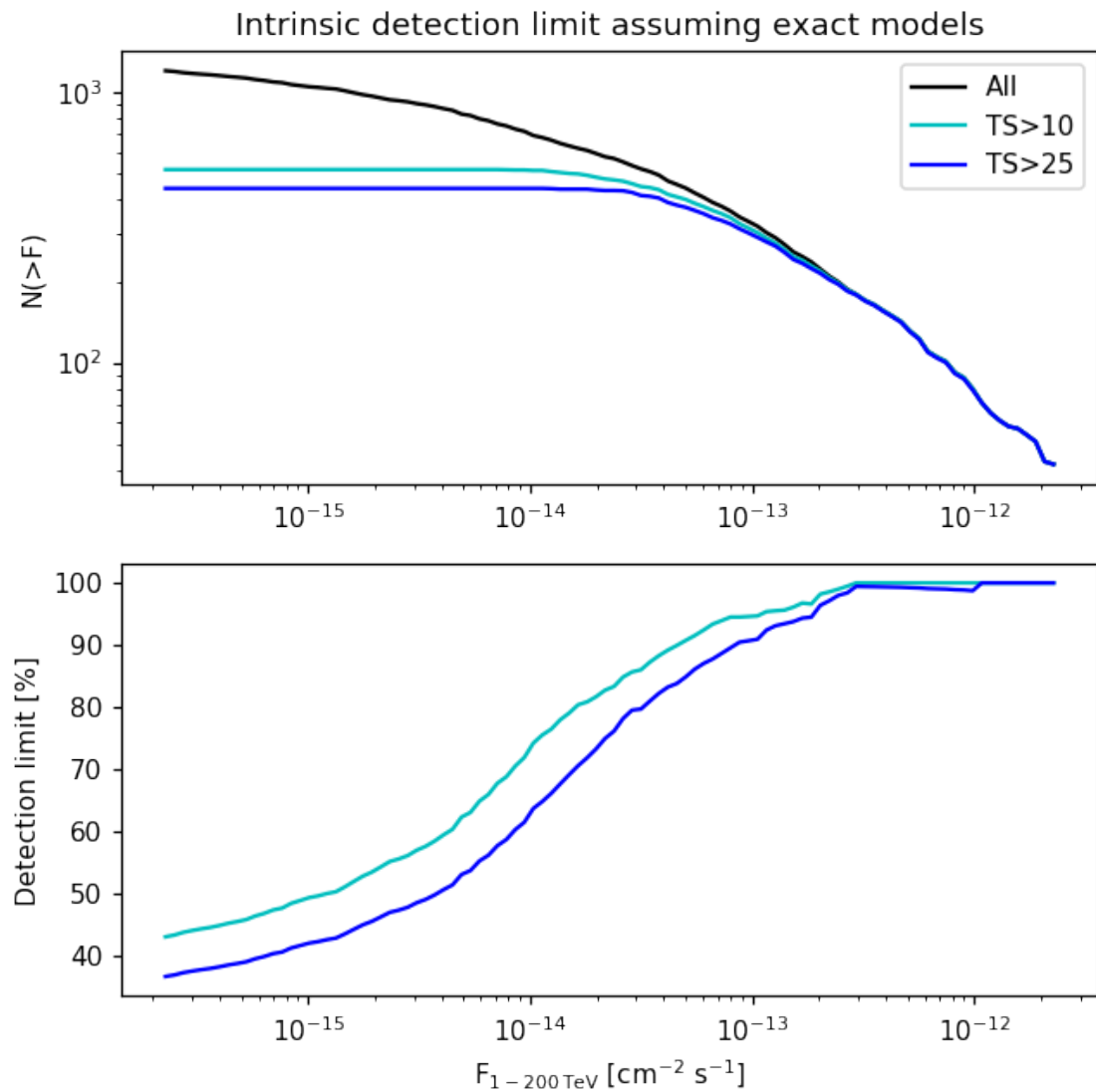


2.2 Detectable sources assuming excat models

```
[336]: # detectable sources
```

Nsource: 1494
 Nsource with TS>10: 519
 Nsource with TS>25: 442

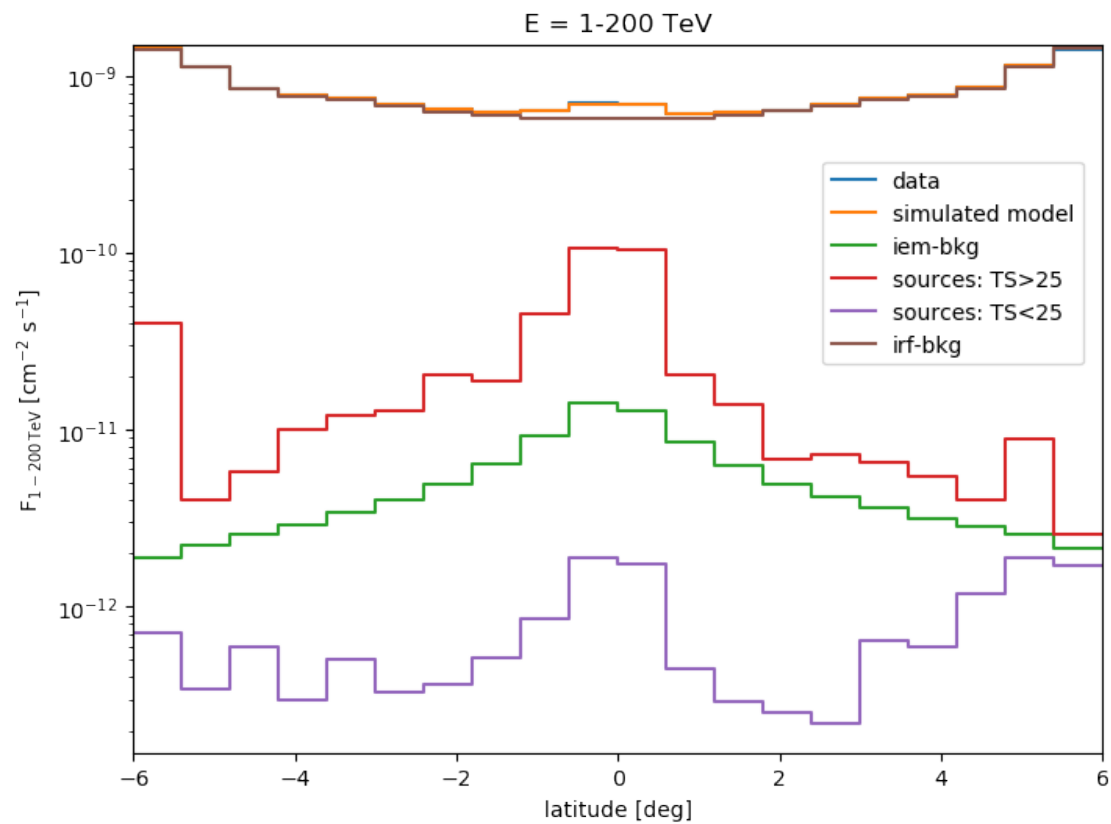
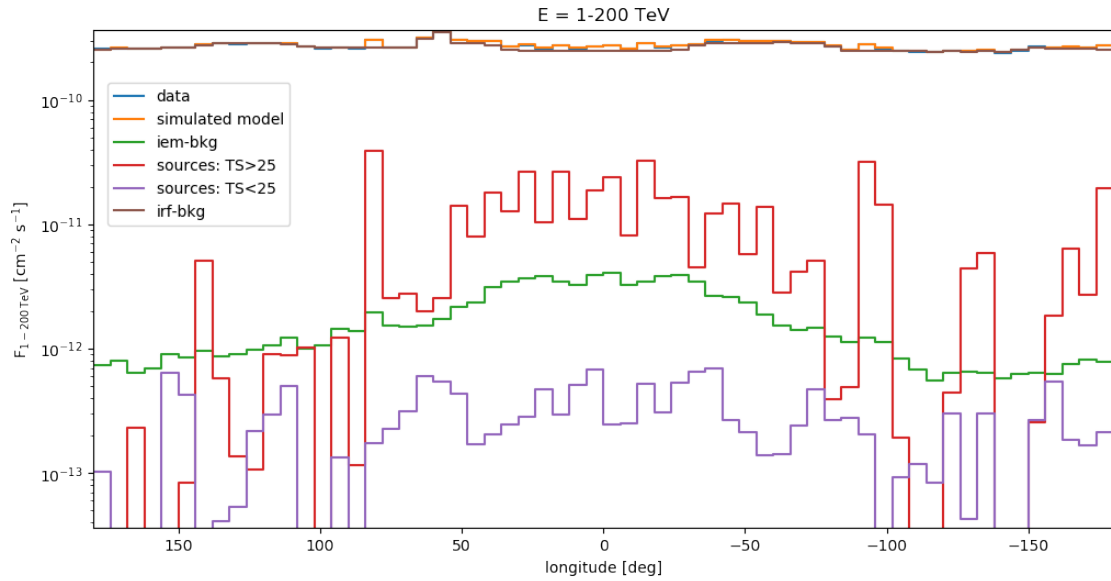
Nsource with TS>30: 425
 Nsource known (TS>25): 127
 Nsource new (TS>25): 315



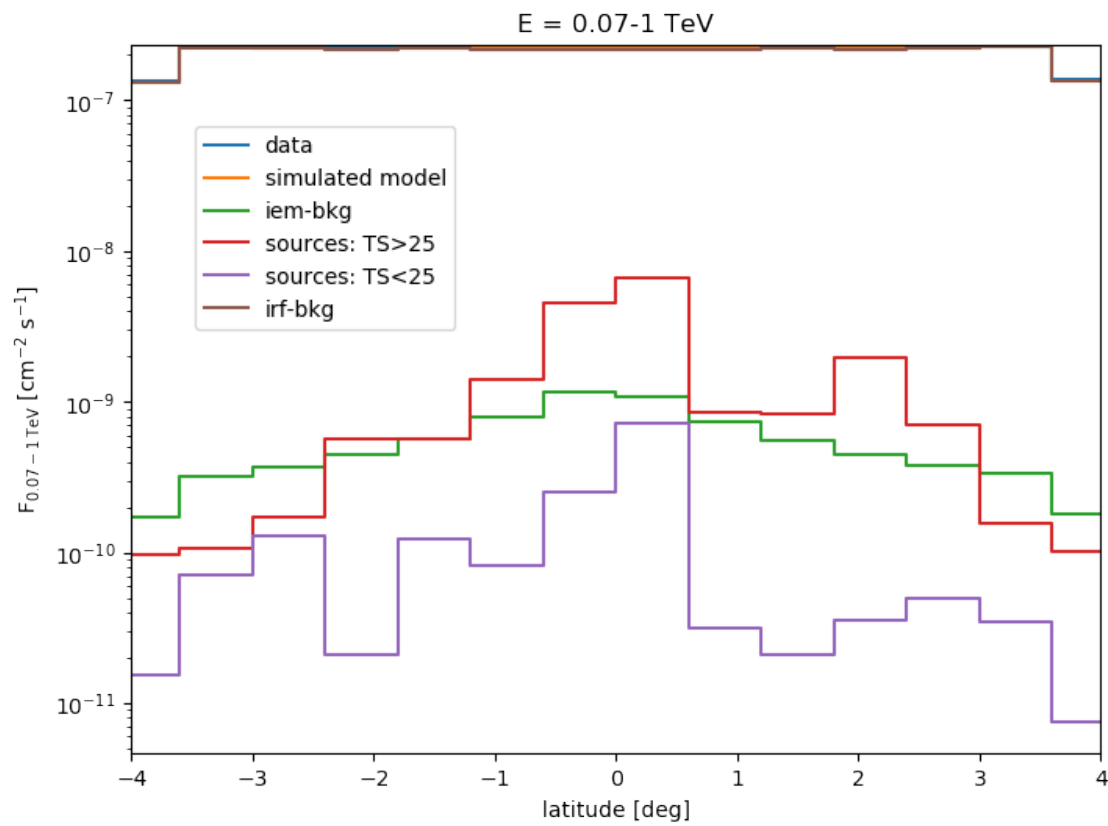
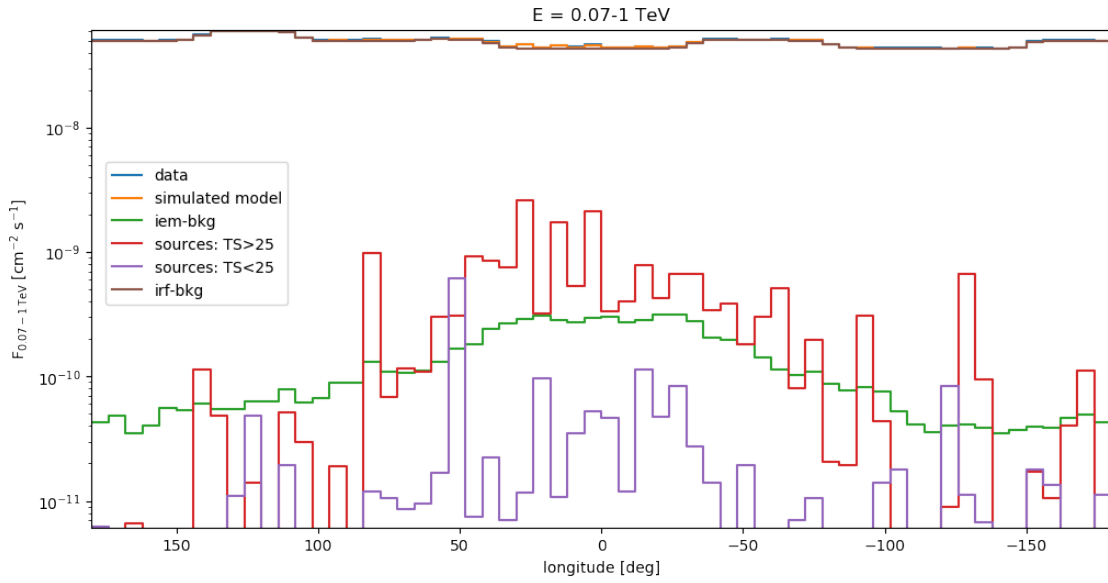
Note : these curves and the numbers of detectable source expected for a given TS are very similar to those computed for the DC-1.

Backgrounds and sources contributions in exact models

[337]: # exact model components postTeV



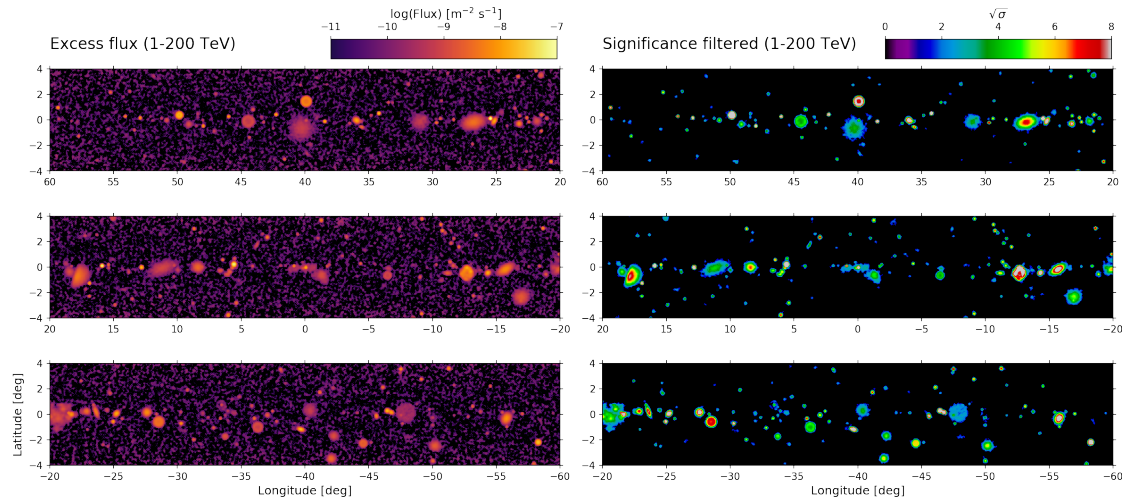
[338]: # exact model components subTeV



3 Detection

3.1 Excess and significance

[339]: `# excess and significance`



3.2 Seed lists

[340]: `# seed lists`

3.3 Outliers detection

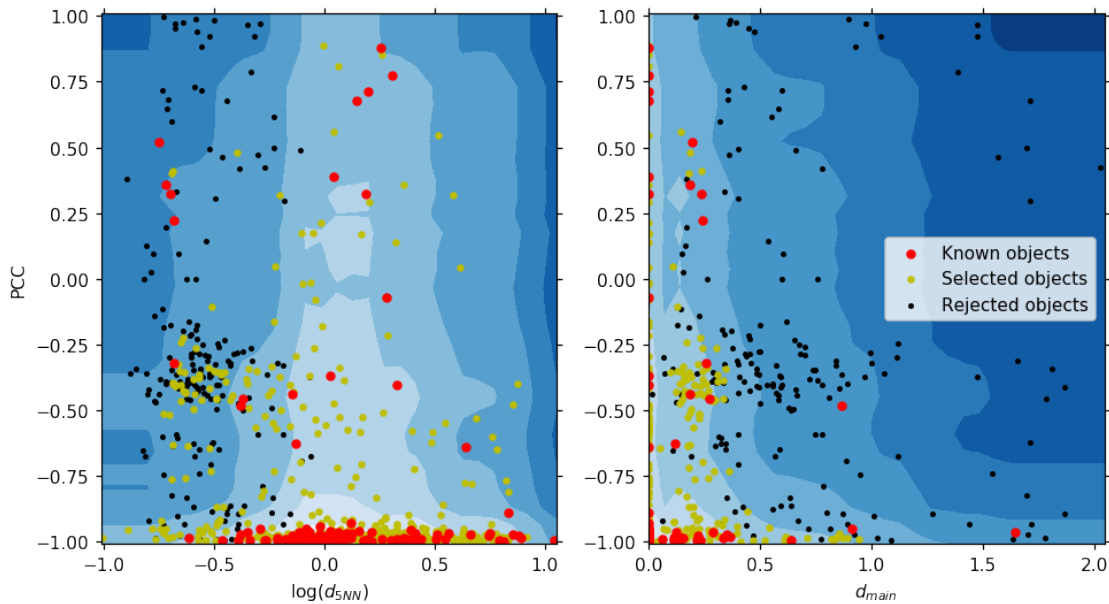
[341]: `# outliers detection`

```
All source
Objects detected: 799
Objects associated (SFOverlap>0.25): 456
Reconstruction fraction (TS>10): 0.76
Reconstruction fraction (TS>30): 0.86
Association fraction: 0.57
Dissimilarity score (TS>30): 0.51
```

```
Known source selection
Objects detected: 120
Objects associated (SFOverlap>0.25): 120
Reconstruction fraction (TS>10): 0.85
Reconstruction fraction (TS>30): 0.87
Association fraction: 1.0
Dissimilarity score (TS>30): 0.13
```

```
Minimal association error 0.03333333333333333  
regular: 497  
anormal: 182  
selected (known+regular): 617
```

```
Candidate sources selection  
Objects detected: 617  
Objects associated (SFoverlap>0.25): 445  
Reconstruction fraction (TS>10): 0.76  
Reconstruction fraction (TS>30): 0.84  
Association fraction: 0.72  
Dissimilarity score (TS>30): 0.39
```



<Figure size 432x288 with 0 Axes>

```
[342]: #score
```

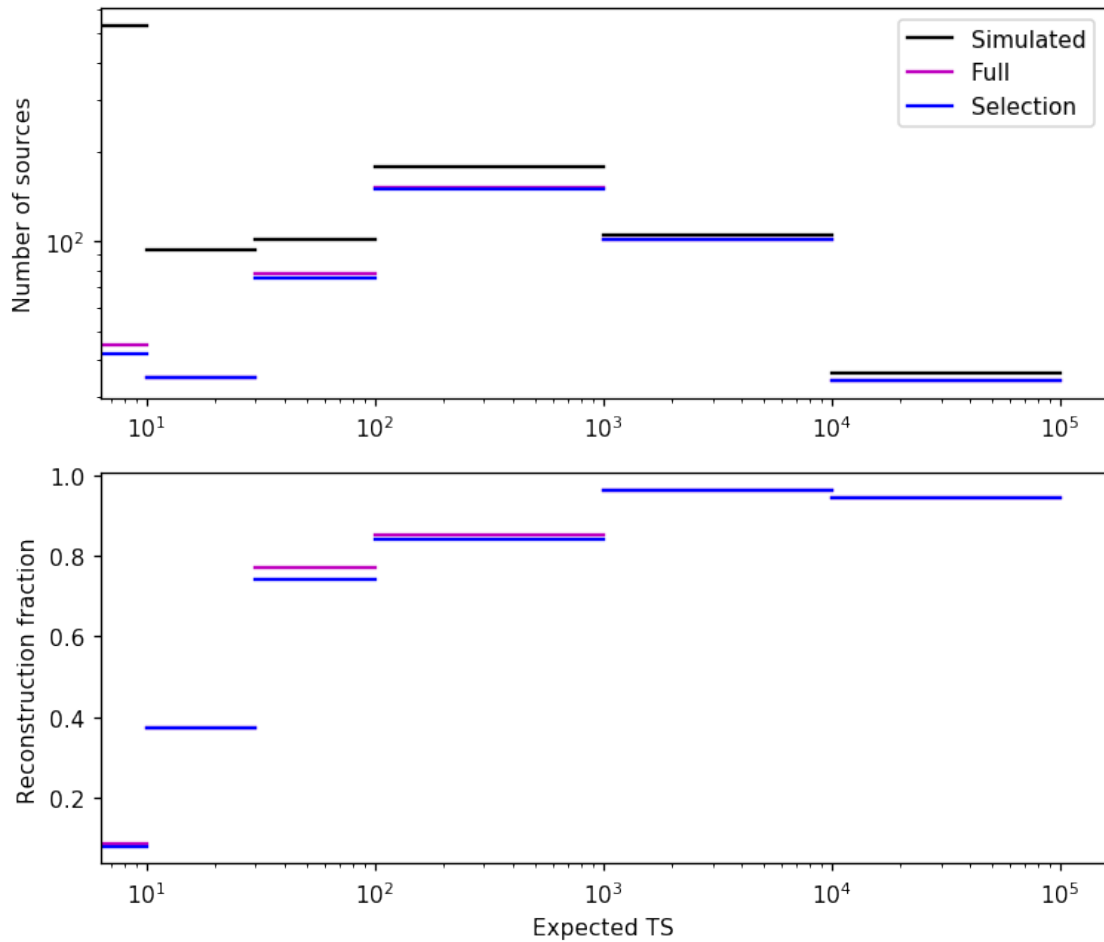
```
Main objects  
Objects detected: 500  
Objects associated (SFoverlap>0.25): 428  
Reconstruction fraction (TS>10): 0.74  
Reconstruction fraction (TS>30): 0.83  
Association fraction: 0.86
```

Dissimilarity score (TS>30): 0.29

Sub-structures
Objects detected: 122
Objects associated ($SF_{overlap} > 0.25$): 18
Reconstruction fraction (TS>10): 0.02
Reconstruction fraction (TS>30): 0.02
Association fraction: 0.15
Dissimilarity score (TS>30): 1.0

3.4 Reconstruction fraction (seed lists)

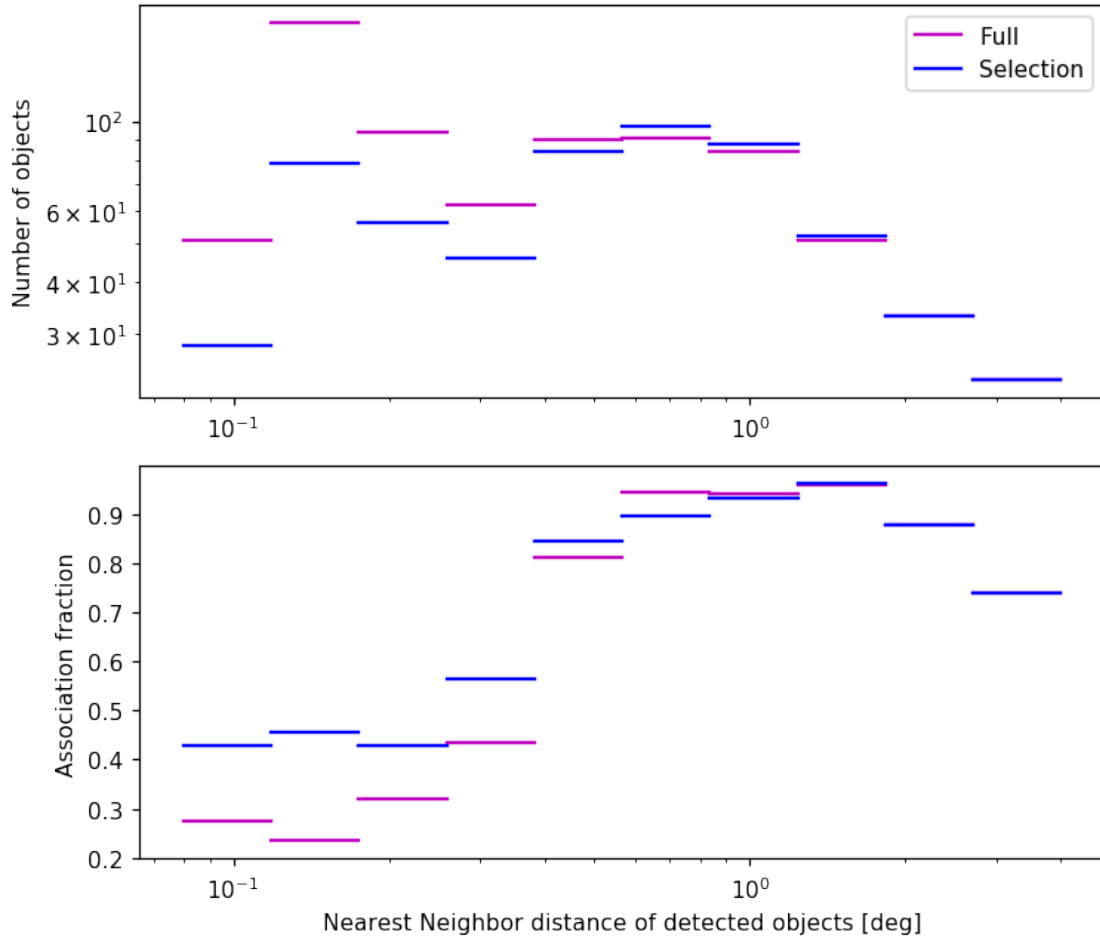
[343]: *# reconstruction fraction*



3.5 Association fraction (seed lists)

```
[344]: # association fraction
```

```
kdist lim: 0.0024185094905847513 6.397523092910374
```

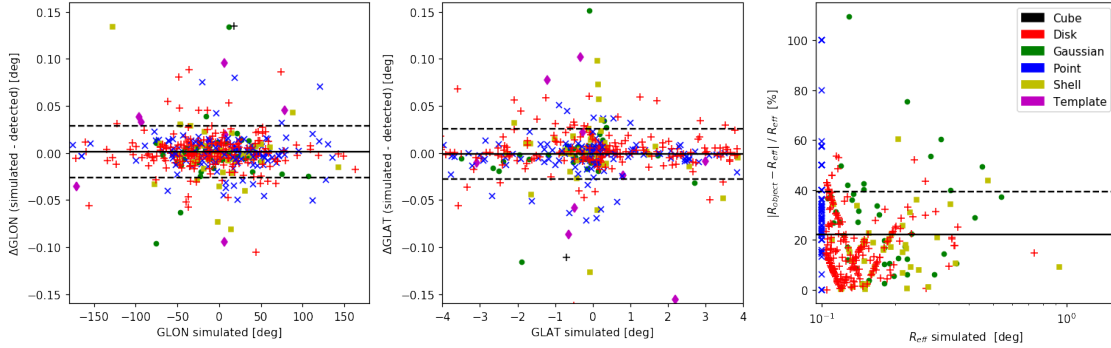


3.6 Position and radius (seeds list)

```
[345]: # match list and simulated/catalogues
```

```
[346]: # position and radius correlations
```

```
Associations correlations
intercenter distance : 0.023546407 +/- 0.030259065
dispersion l [deg]: 0.001219054 +/- 0.027471416
dispersion b [deg]: -0.00082664215 +/- 0.026705733
dispersion r [deg]: -0.008554664039957588 +/- 0.04203883605038287
relative error r [%]: 0.223159751803078 +/- 0.1689384217972307
```



Note : For the seed lists, objects are detected on significance maps with a correlation radius R_{corr} , we can not compare directly their radius to those of known sources (simulated or catalogued). So for each known source we introduce an effective radius as $R_{eff} = \sqrt{R_{source}^2 + R_{corr}^2}$. We define R_{source} as the outer radius for shell-like sources, the 1σ width for Gaussian-like sources, the radius for disk-like sources, and zero for point-like sources.

4 Fit results

4.1 Global model

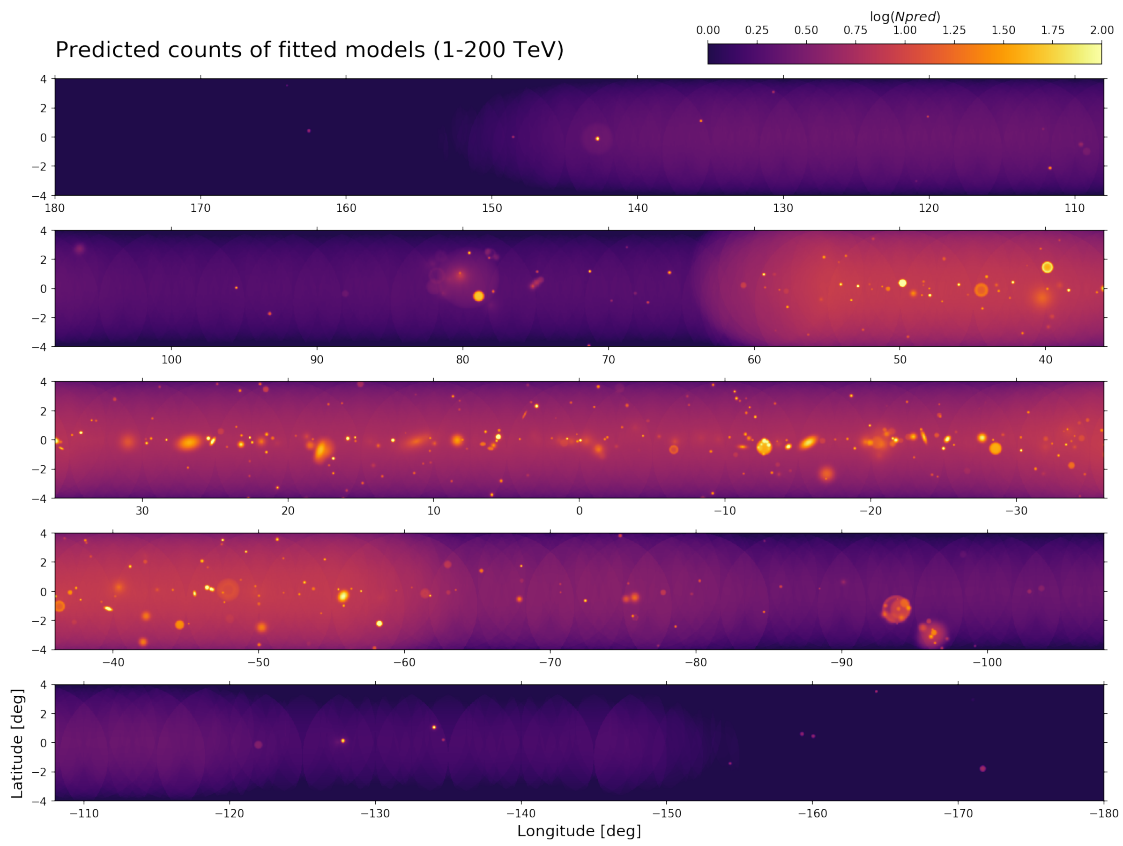
```
[347]: # build global datasets
```

```
[347]: <Table length=5>
```

Name	GLON	err_GLON	GLAT	...	TSnull	TSbkg	TSall
bytes20	float32	float32	float32	...	float32	float32	float32
-----	-----	-----	-----	...	-----	-----	-----
Seed_52	357.94894	0.020923635	-5.775845	...	-4804.1343	nan	nan
Seed_318	1.1700281	0.009585358	-4.7481656	...	109.50203	nan	nan
Seed_1	5.5806518	0.00021817007	0.20216583	...	580998.94	nan	nan
Seed_54	2.96555828	0.00011461884	2.3212903	...	1152085.0	nan	nan
Seed_63	6.026622	0.001208253	-3.7875636	...	4539.224	nan	nan

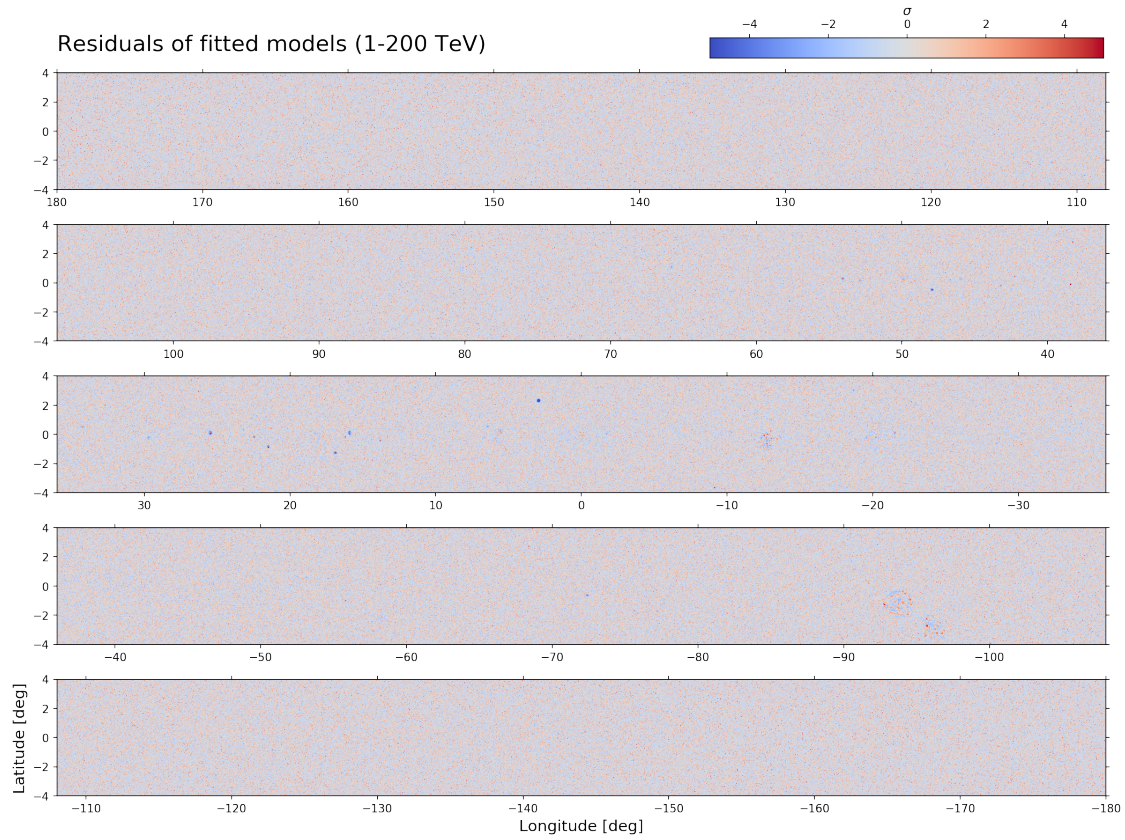
4.1.1 Npred maps

```
[348]: # predicted counts (fitted models)
```

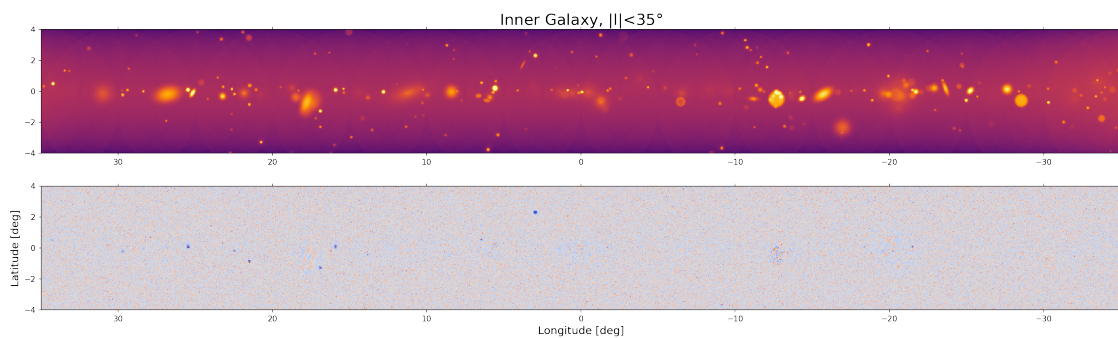


4.1.2 Residuals maps

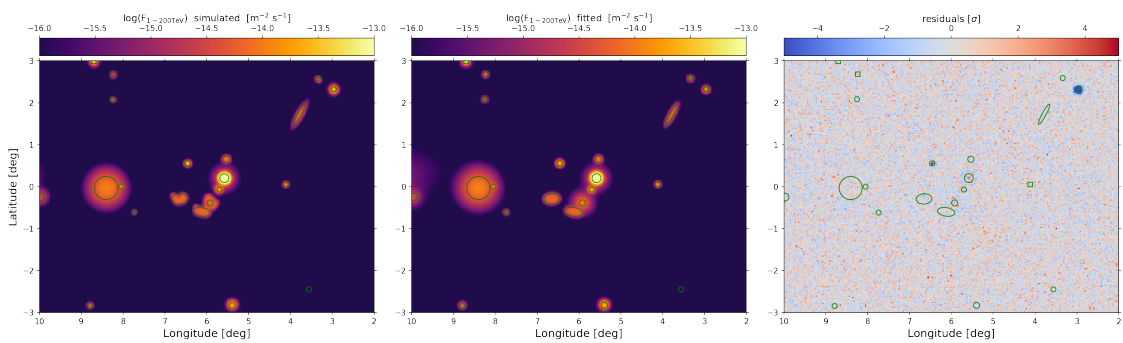
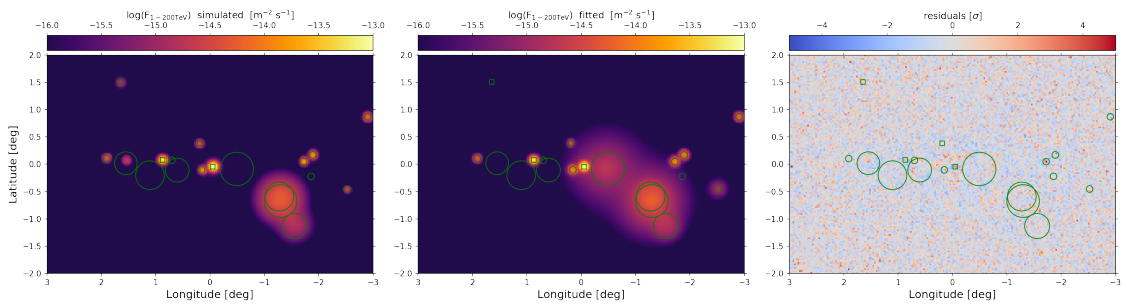
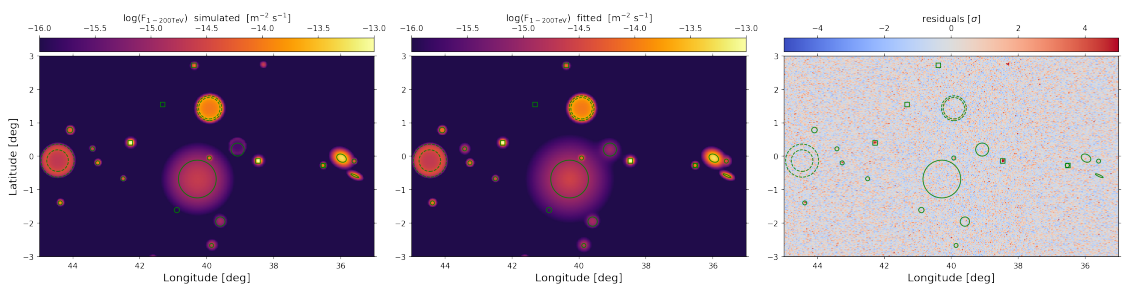
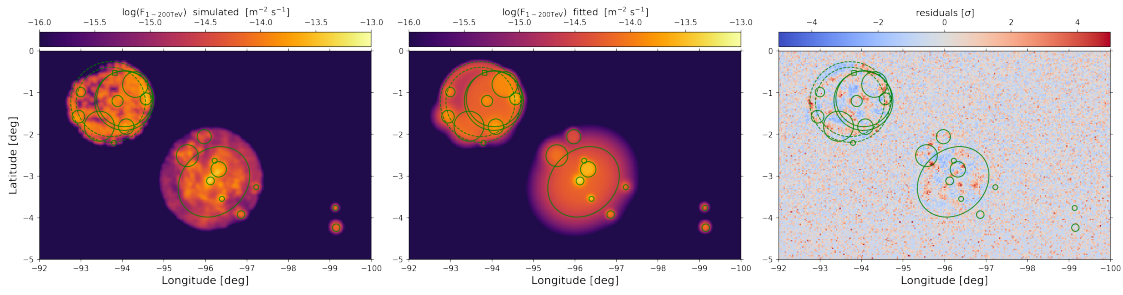
```
[349]: # residuals (fitted models)
```



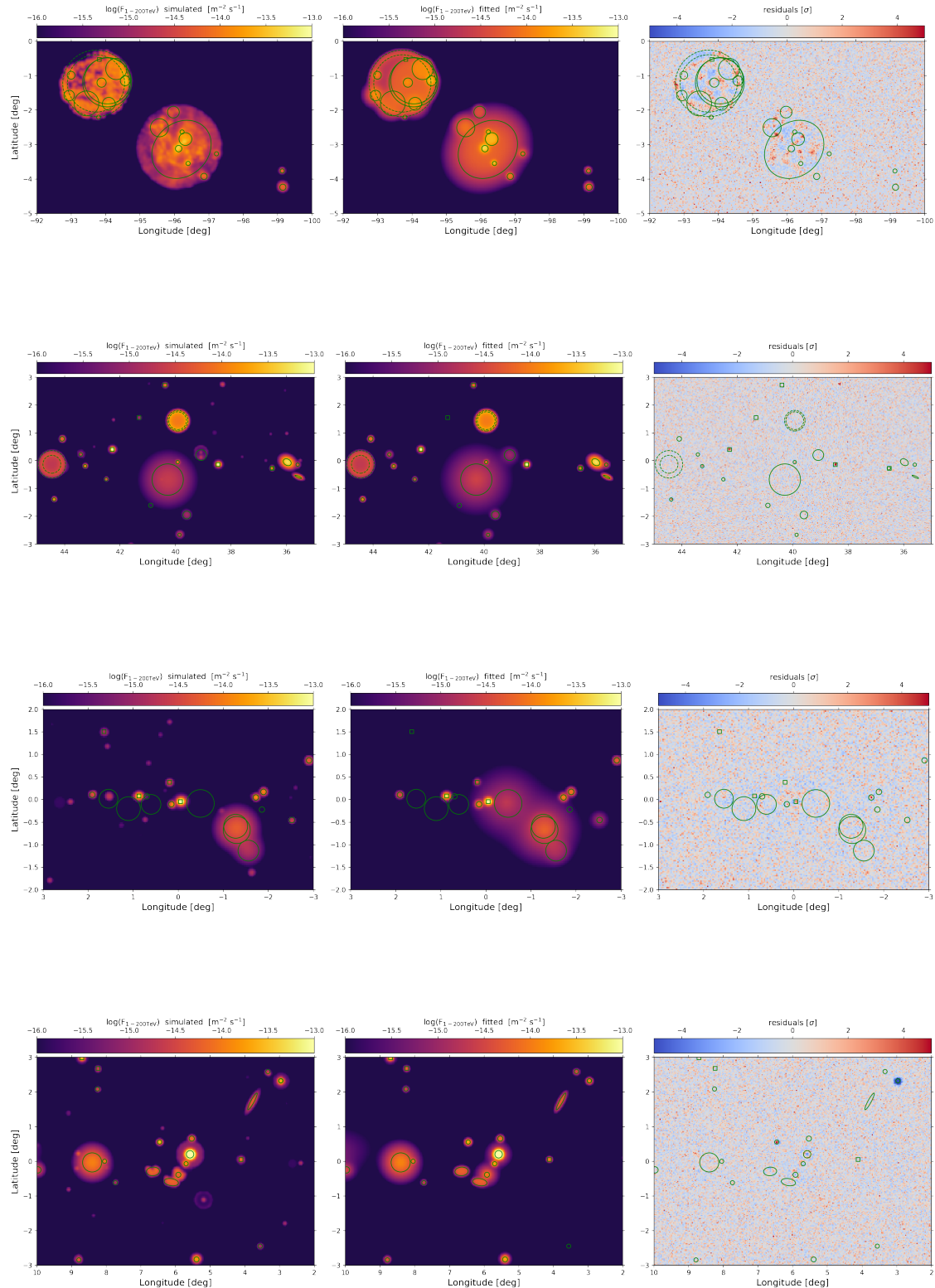
[350]: **### Zoom**



[351]: **### focus comparisons with expected source with TS >25 contribution only**

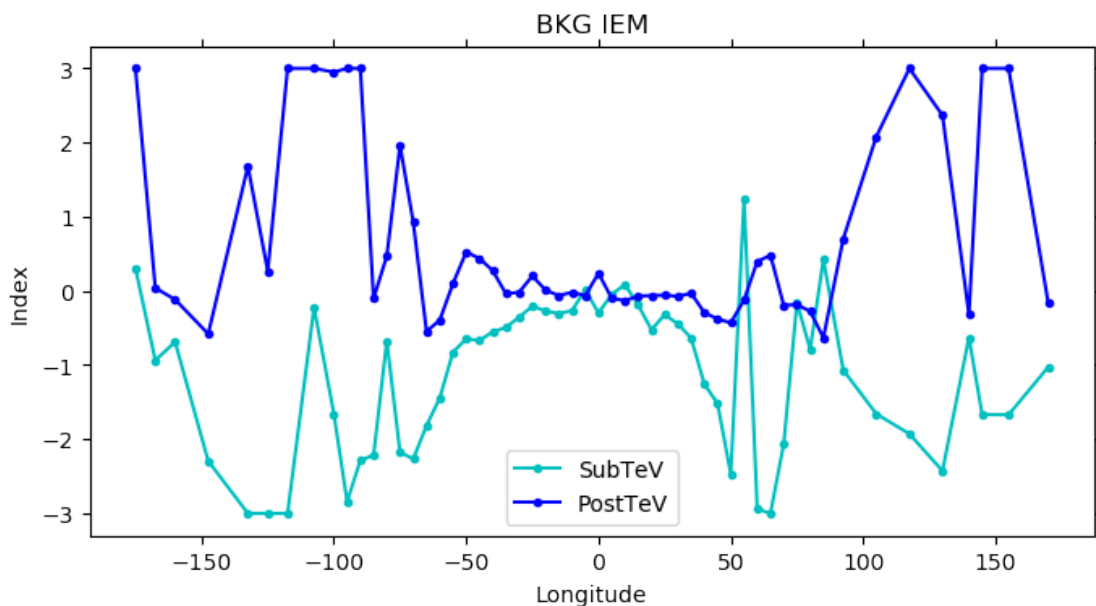
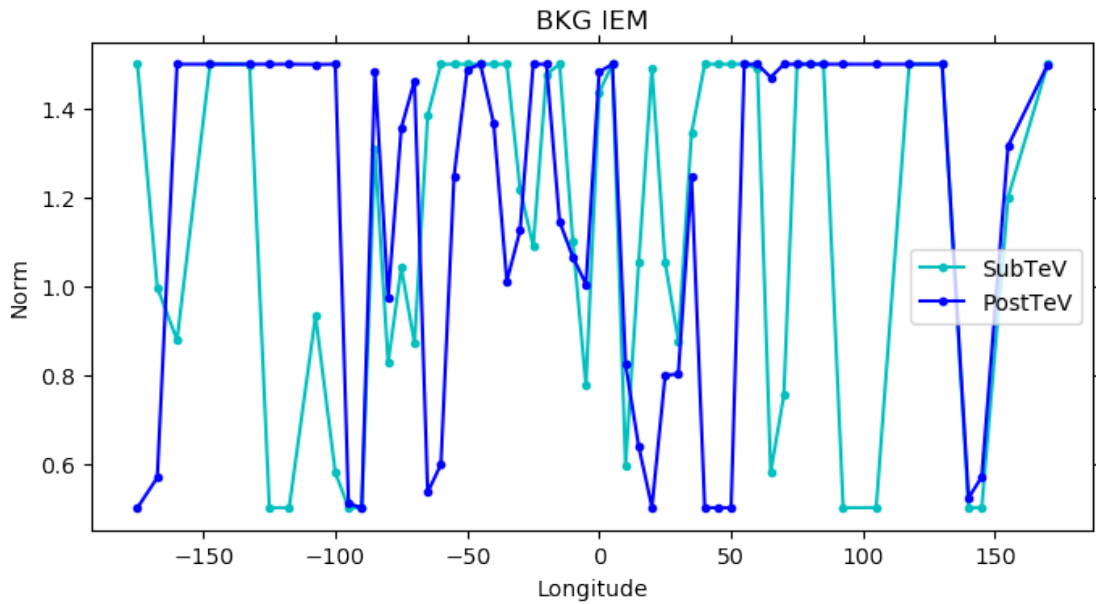


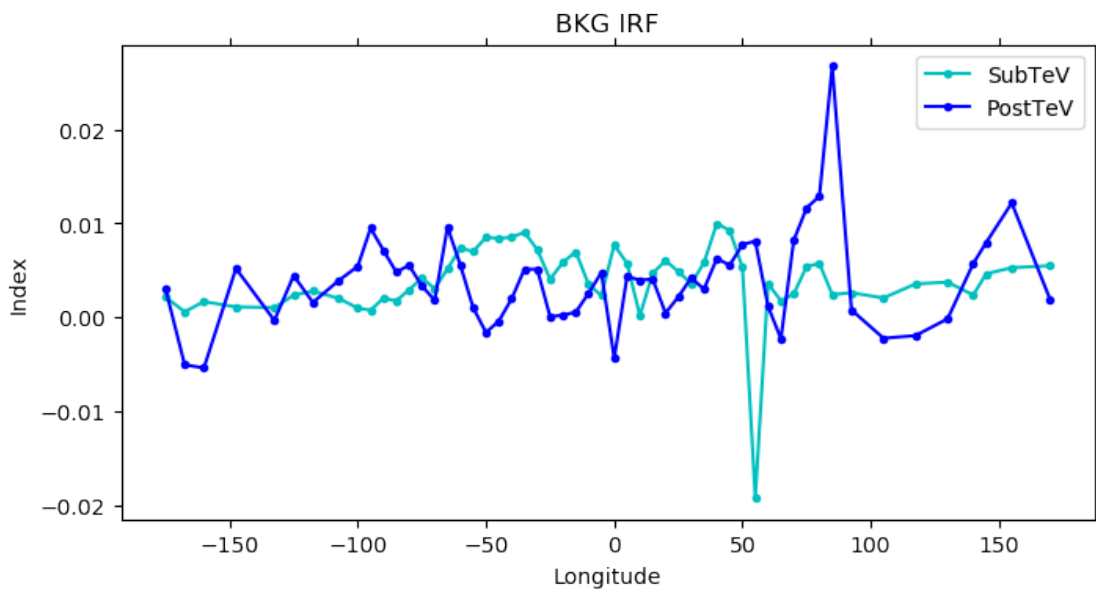
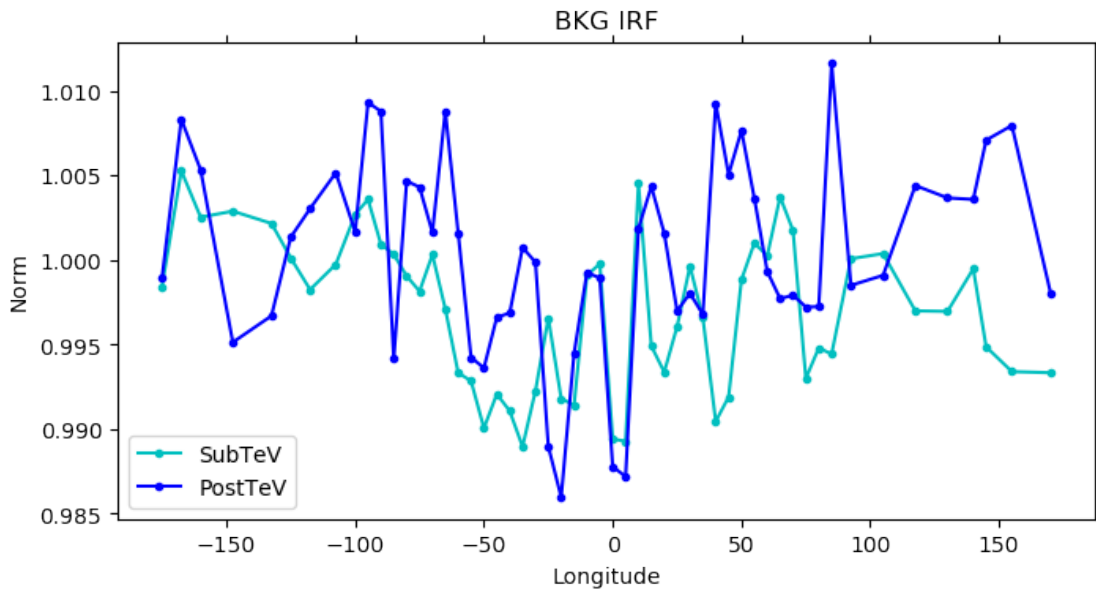
[352]: *### focus comparisons with all expected source*



4.2 Backgrounds parameters

```
[353]: # bkg correction from regions to the global model
```





4.3 Fitted list quality

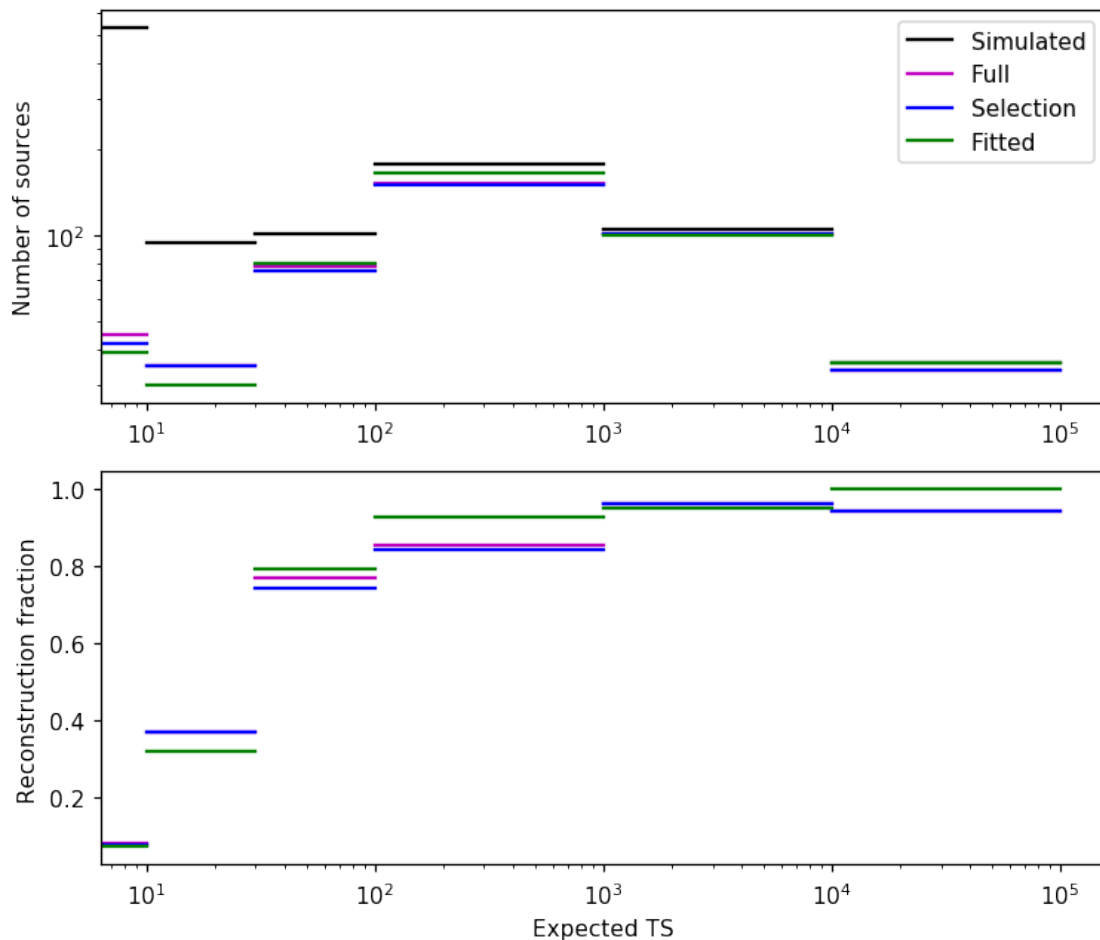
```
[354]: # score
```

Fitted sources

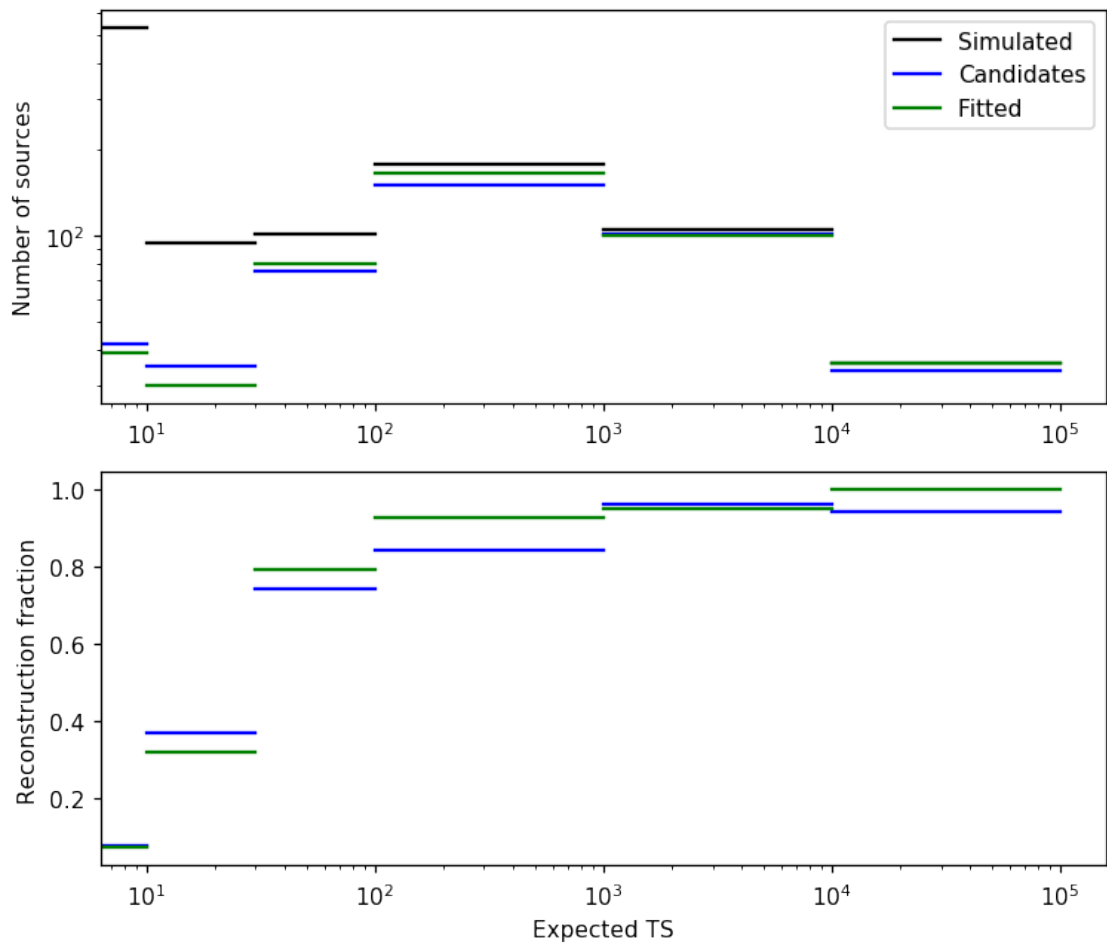
```
Objects detected: 526
Objects associated (SFOverlap>0.25): 434
Reconstruction fraction (TS>10): 0.77
Reconstruction fraction (TS>30): 0.88
Association fraction: 0.83
Dissimilarity score (TS>30): 0.27
```

4.3.1 Reconstruction fraction

```
[355]: #reconstruction fraction
```

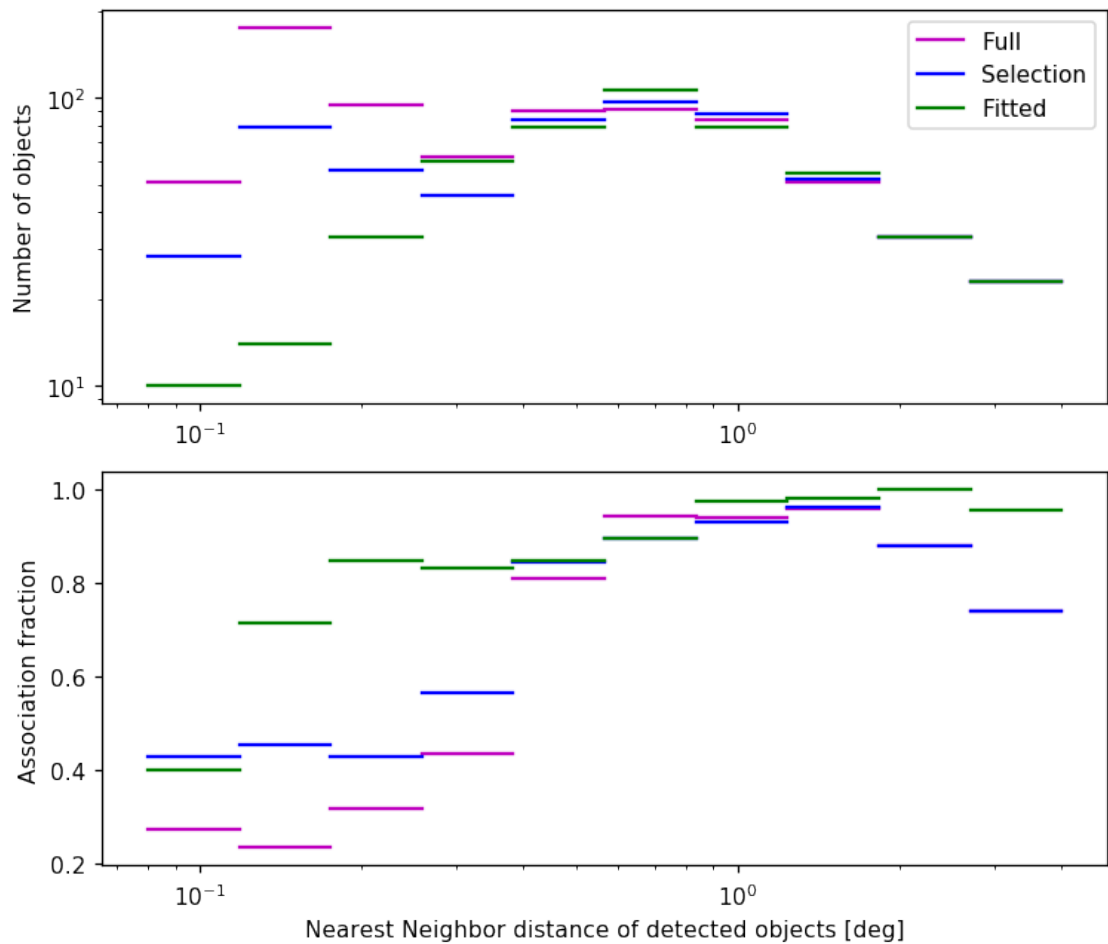


```
[356]: #reconstruction fraction
```

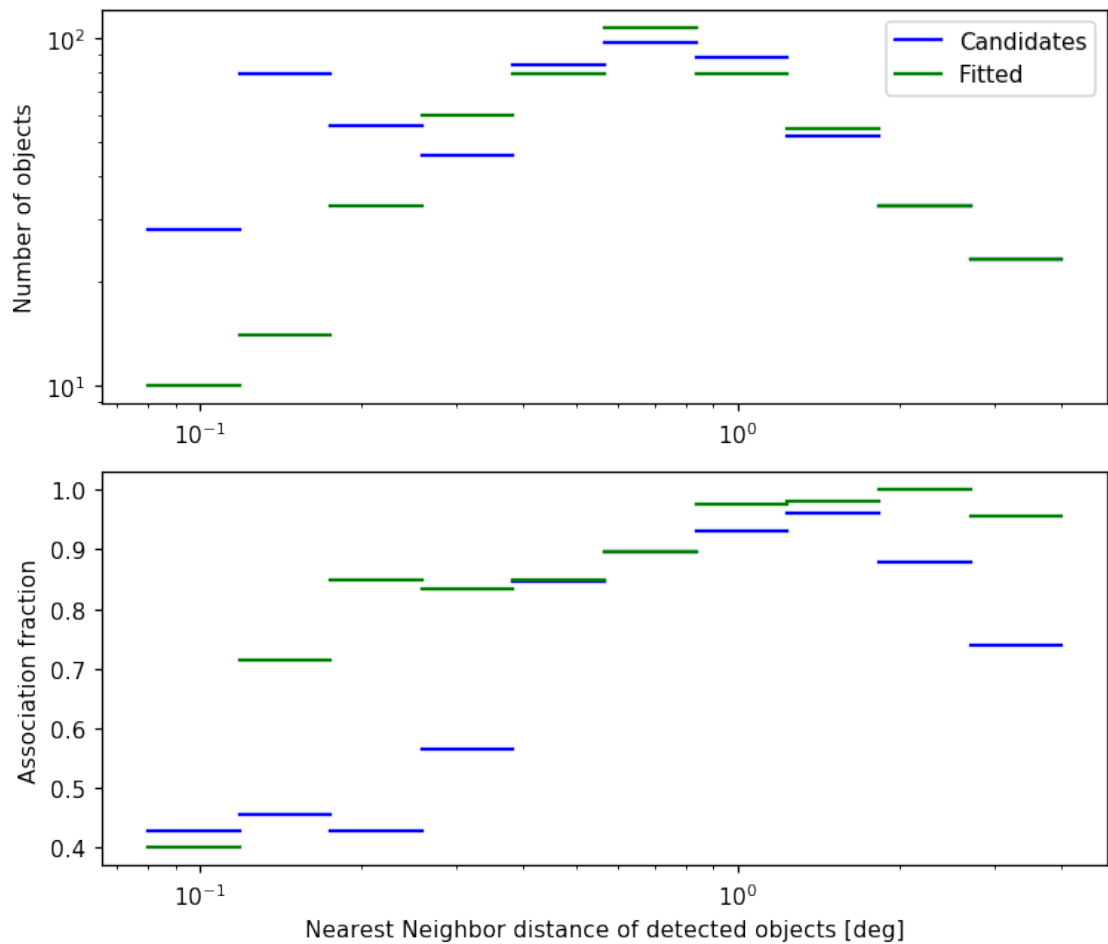


4.3.2 Association fraction

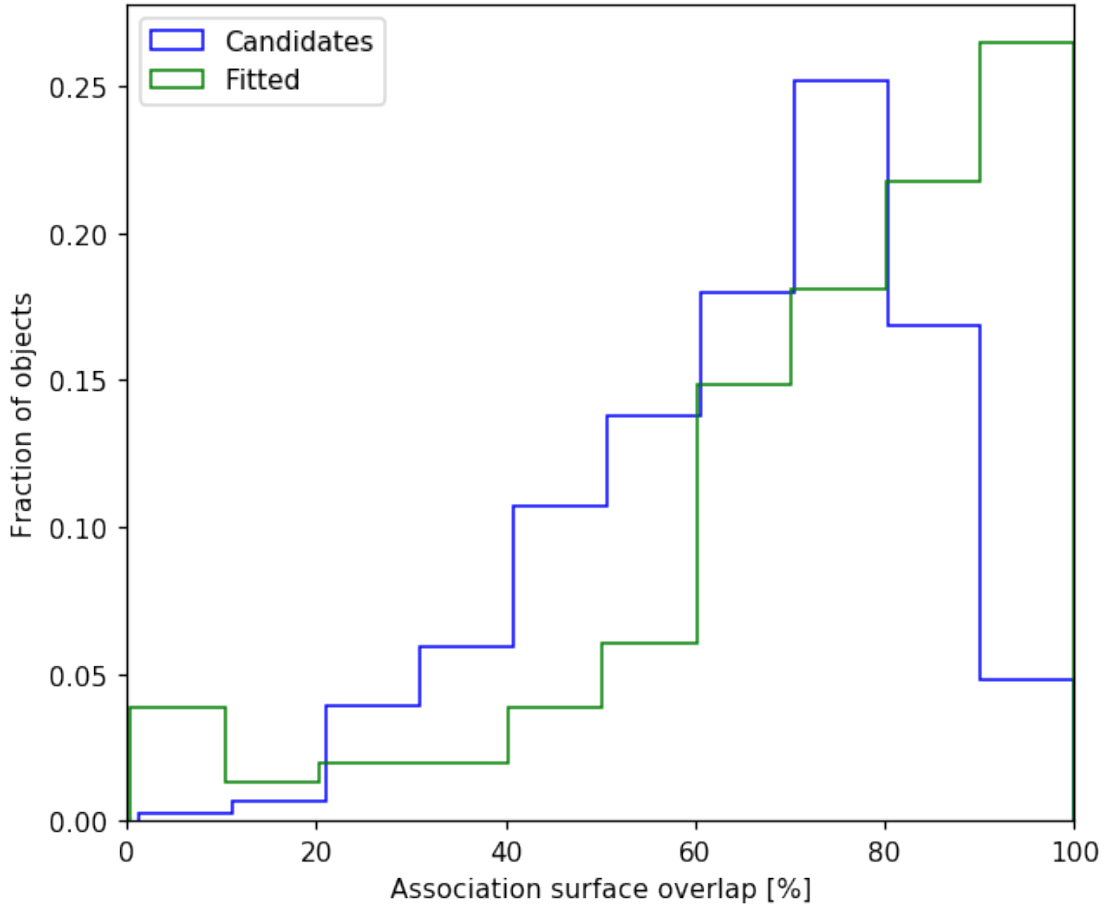
```
[357]: # association fraction
```



[358]: `# association fraction`



[359]: # Association surface overlap distribution



Note : As expected the fit improves the match in spatial models which result in an enhanced association quality as given by the surface overlap criterion

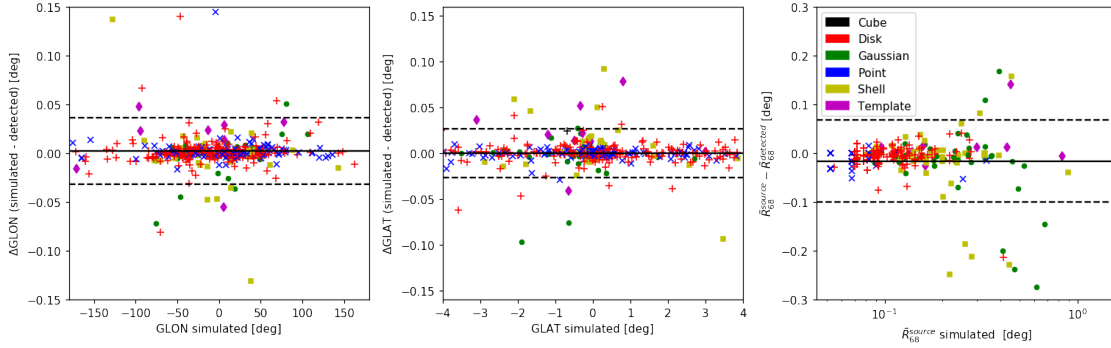
4.4 Parameters correlation for associated sources

```
[360]: # match fitted list and simulated/catalogues
```

4.4.1 Position and radius

```
[361]: # position and errors (fitted models)
```

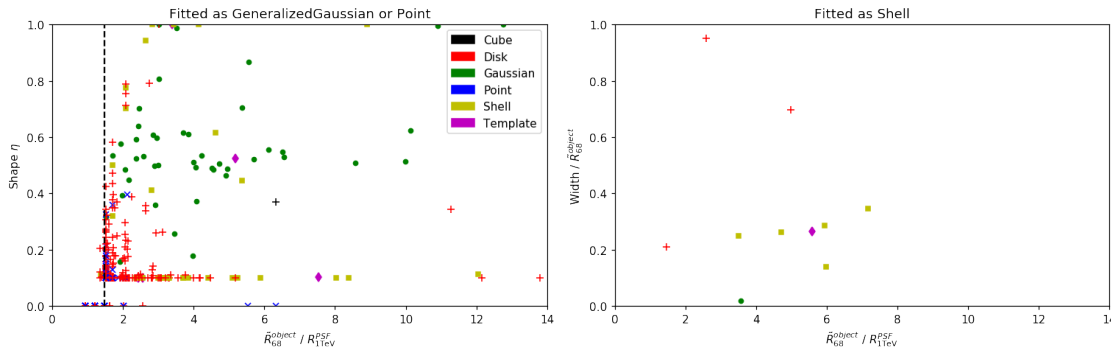
```
Associations correlations
intercenter distance : 0.015649848 +/- 0.04043498
dispersion l [deg] : 0.00245726 +/- 0.034198385
dispersion b [deg] : -0.0001971837 +/- 0.026538633
dispersion r [deg] : -0.016045852 +/- 0.08379901
relative error r [%] : 0.15218991895009368 +/- 0.23064013513575513
```



Notes : In order to compare all source models consistently we use the 68 containment radius of the psf-convolved source flux, noted \tilde{R}_{68} (otherwise simulated template or point sources sources don't have a radius parameter defined).

4.4.2 Morphology : shape parameters

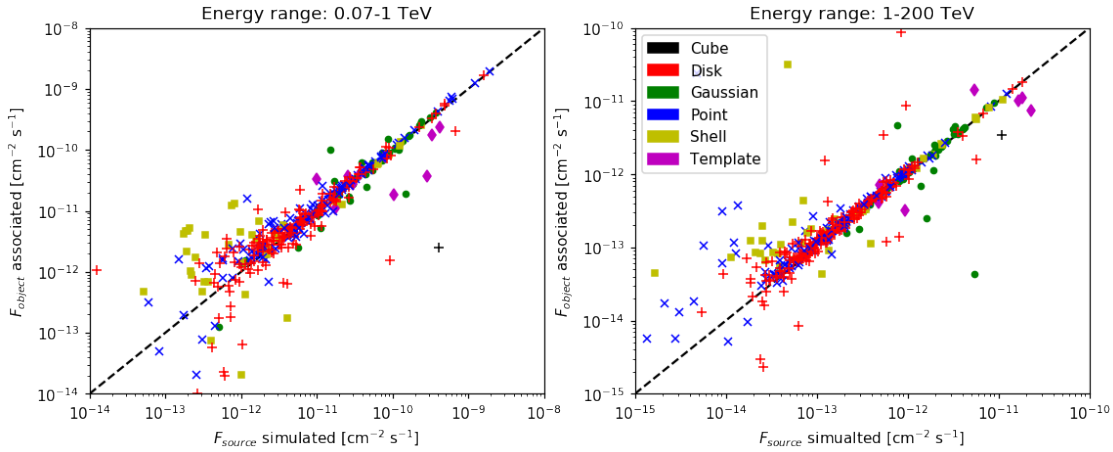
[362]: *# morphological shape*



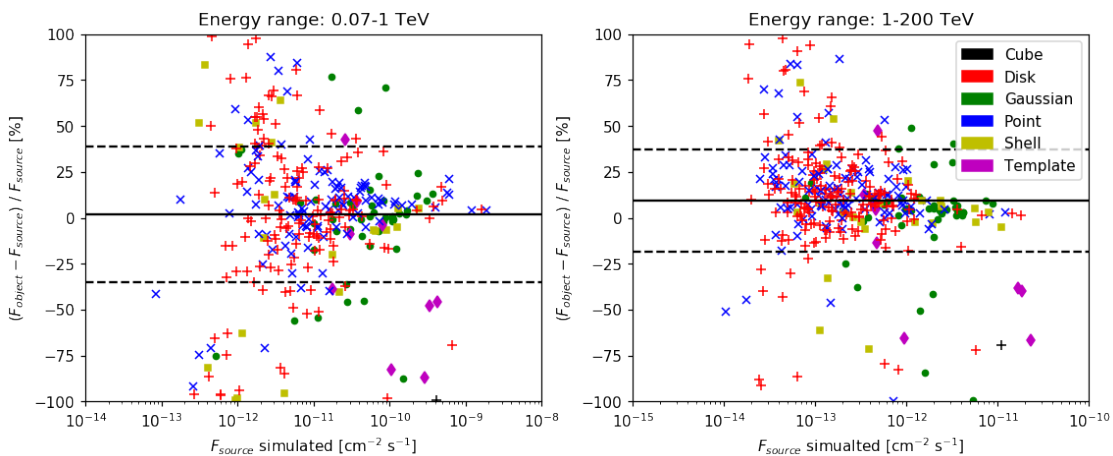
Note : By definition the generalized gaussian effective radius fitted do not match exactly the simulated source radius, we have also to consider shape parameter of the object. For example $\eta=0.5$ is equivalent to a gaussian, in that case $R_{\text{eff}} = \sqrt{2}\sigma$. In this plot we see that most of the gaussian source are reconstructed with η close to 0.5 as expected. The dotted vertical line is the quadratic sum of the minimal radius with the psf radius at 1 TeV relative to the psf radius.

4.4.3 Flux

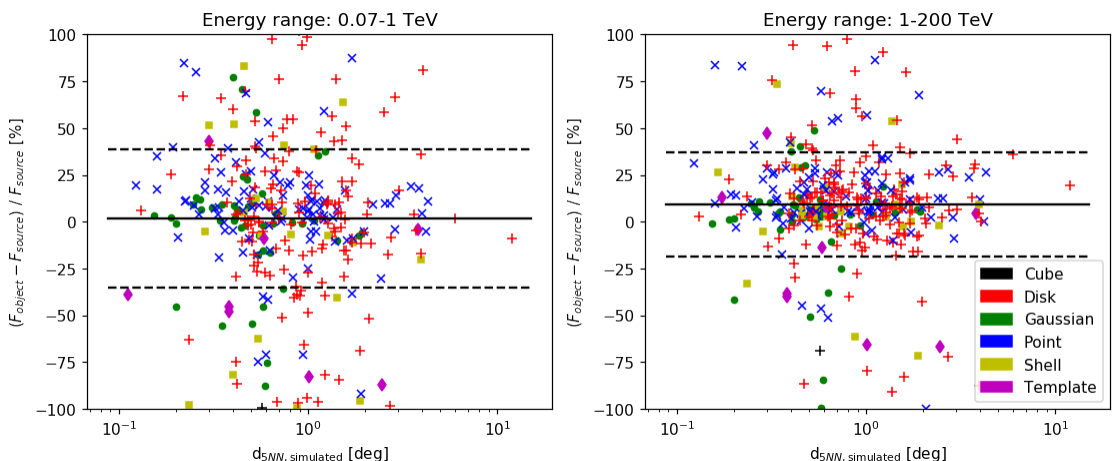
[363]: *# flux correlations*



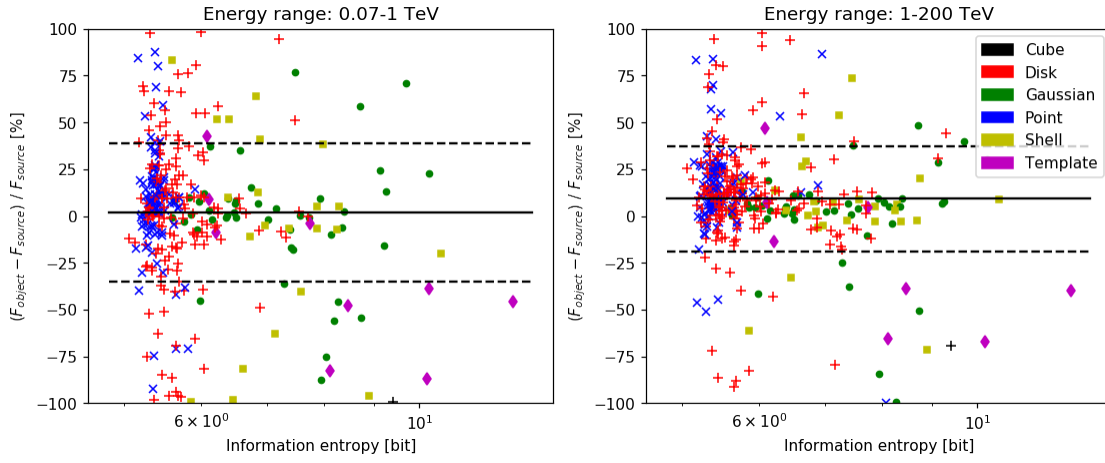
[364]: # flux relative error



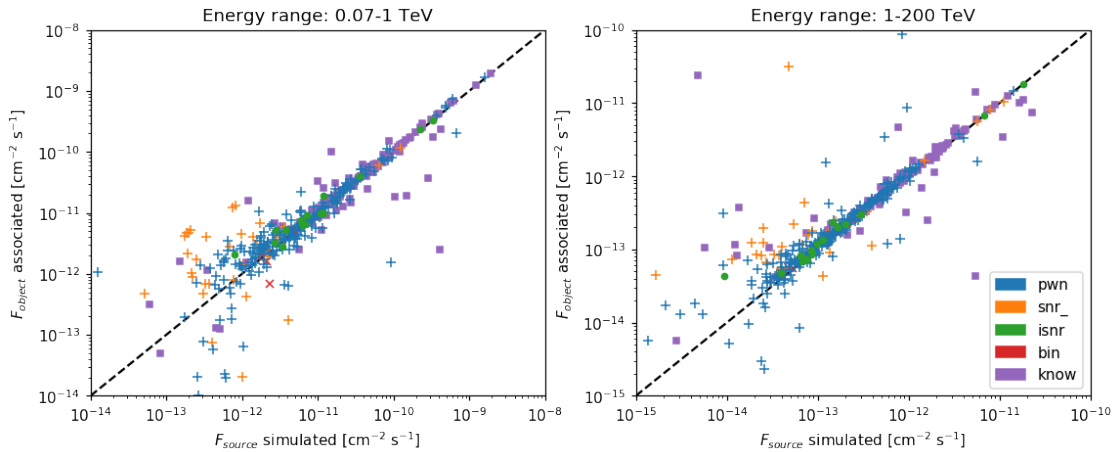
[365]: # flux relative error vs nearest neighbor distance



[366]: # flux relative error vs information entropy



[367]: # flux correlations pop

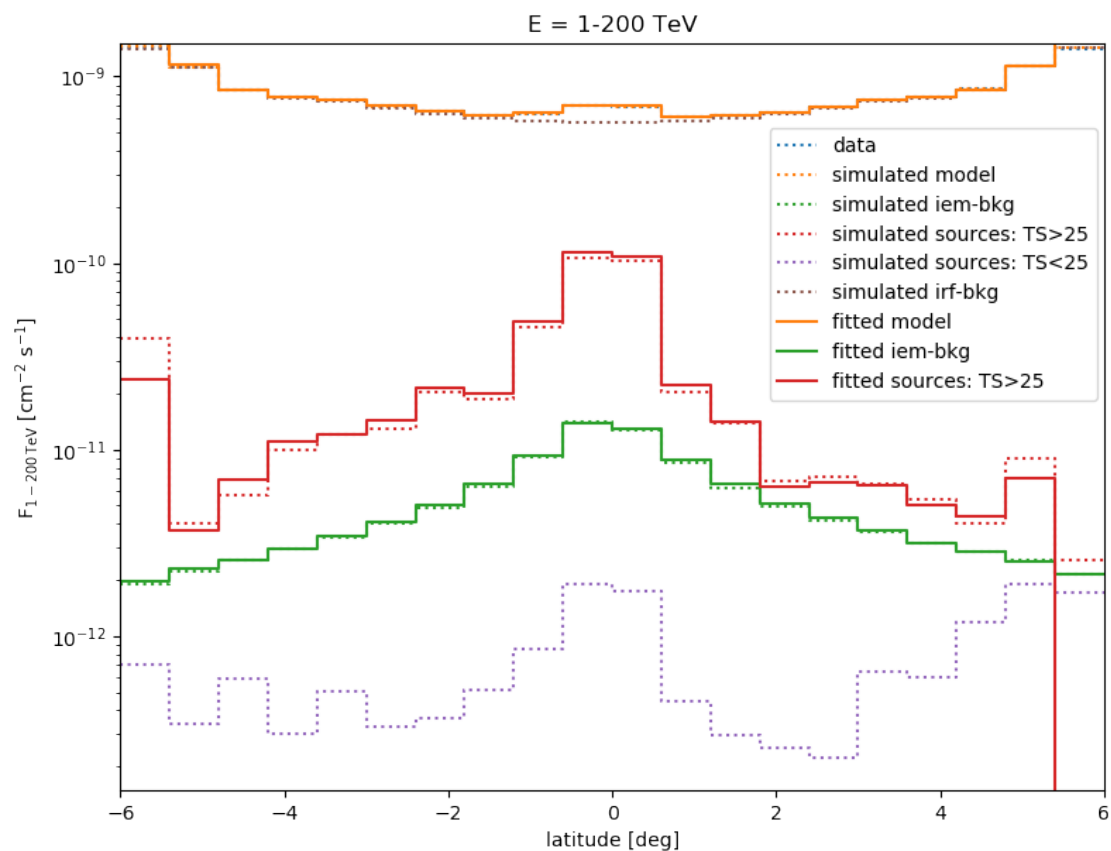
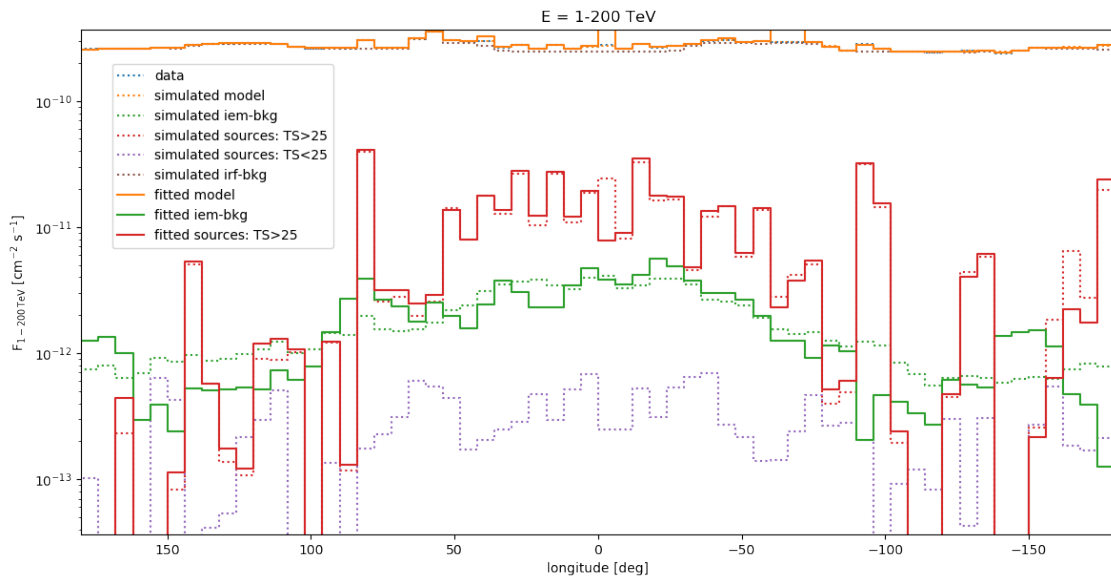


Note : The flux of complex sources (template or elliptical) is under-estimated if we consider unique associations.

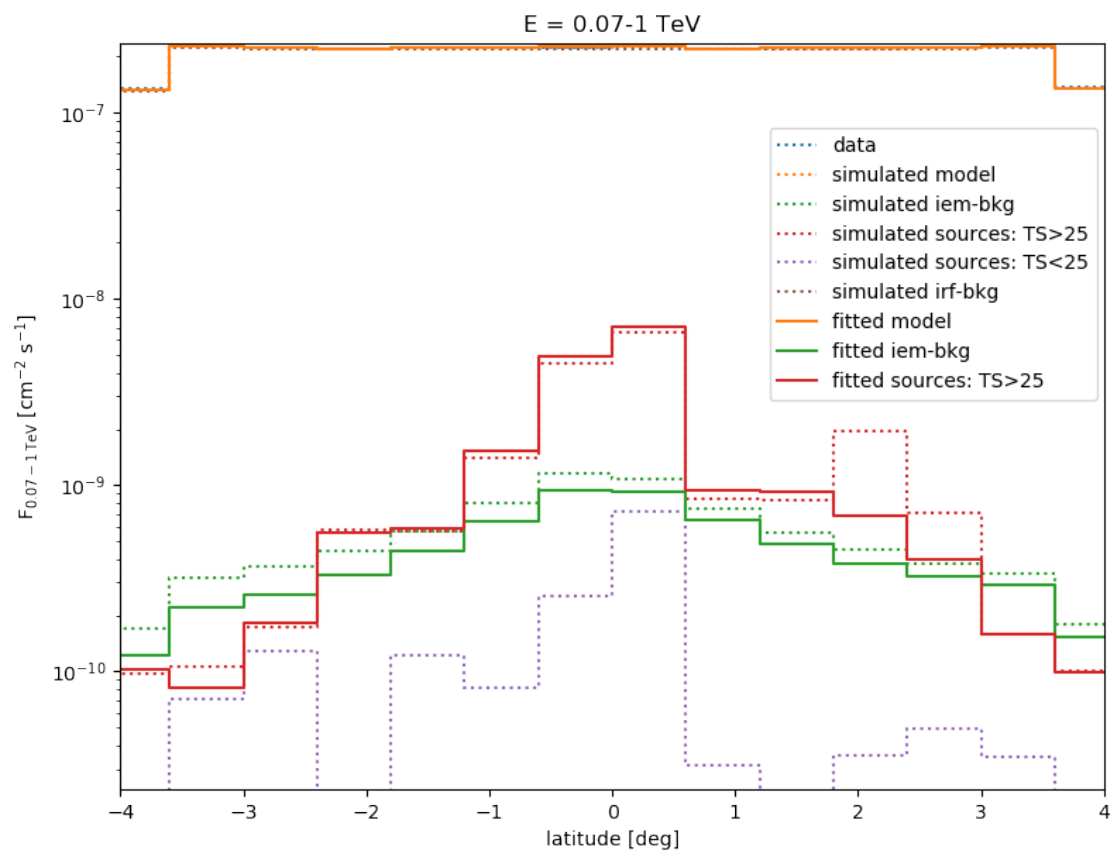
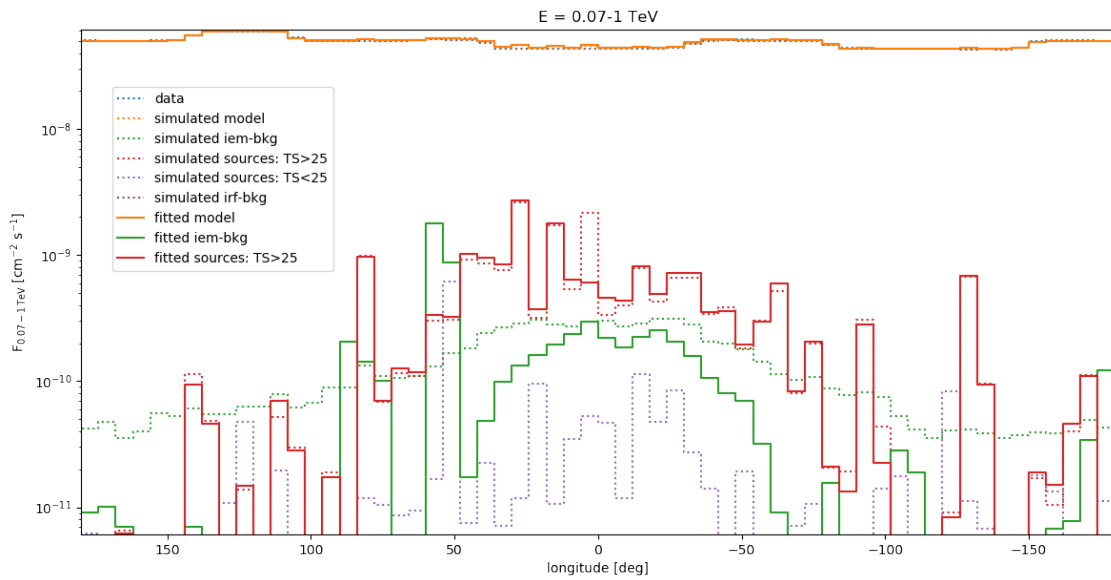
Have to do the same plot including main+sub-structures after merging decisions, maybe considering all sub-structures not associated to others and of similar spectrum only.

Same remark for the logN-logS in next sub-section.

[368]: # fitted model components postTeV



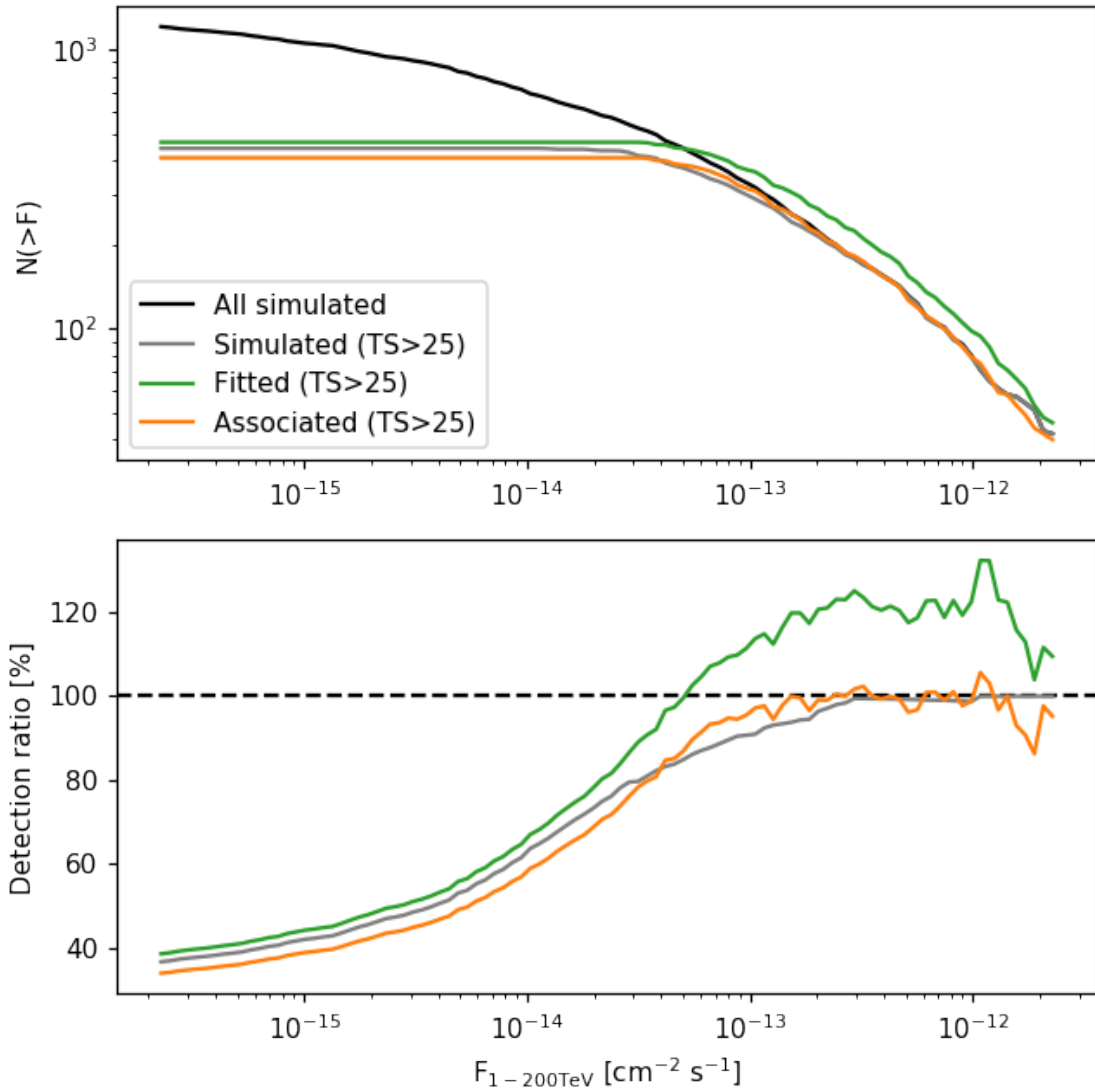
[369]: `# fitted model components subTeV`



4.4.4 logN-logS

[370]: `#logN-logS and detection ratio`

```
Nsource simulated with TS>25 (for E = 1-200 TeV): 442
Nsource fitted with TS>25 (for E = 1-200 TeV): 465
Nsource associated with TS>25 (for E = 1-200 TeV): 409
```



Note : There is potential reasons for the positive biases that are not really false detections:

- in the low-flux regime, the flux and TS of sources near threshold are probably enhanced due to the sea of weaker sources (Eddington bias)

- in the high-flux regime, the known sources well-resolved that are simulated with complex templates cannot be modelled with a unique simple shape (elliptical models also cause ambiguities). So the sub-structures create additional detections of lower flux, while the main object that is associated have an under-estimated flux. It could be improved by merging the sub-structures to have a better estimate of flux and number of objects. This extra step to balance the complexity bias should be investigated carefully as it can lead to merge unrelated sources and introduces more negative bias.

[371]: `# logN-logS and reconstruction fraction with condition`

[372]: `# logN-logS and reconstruction fraction per population`

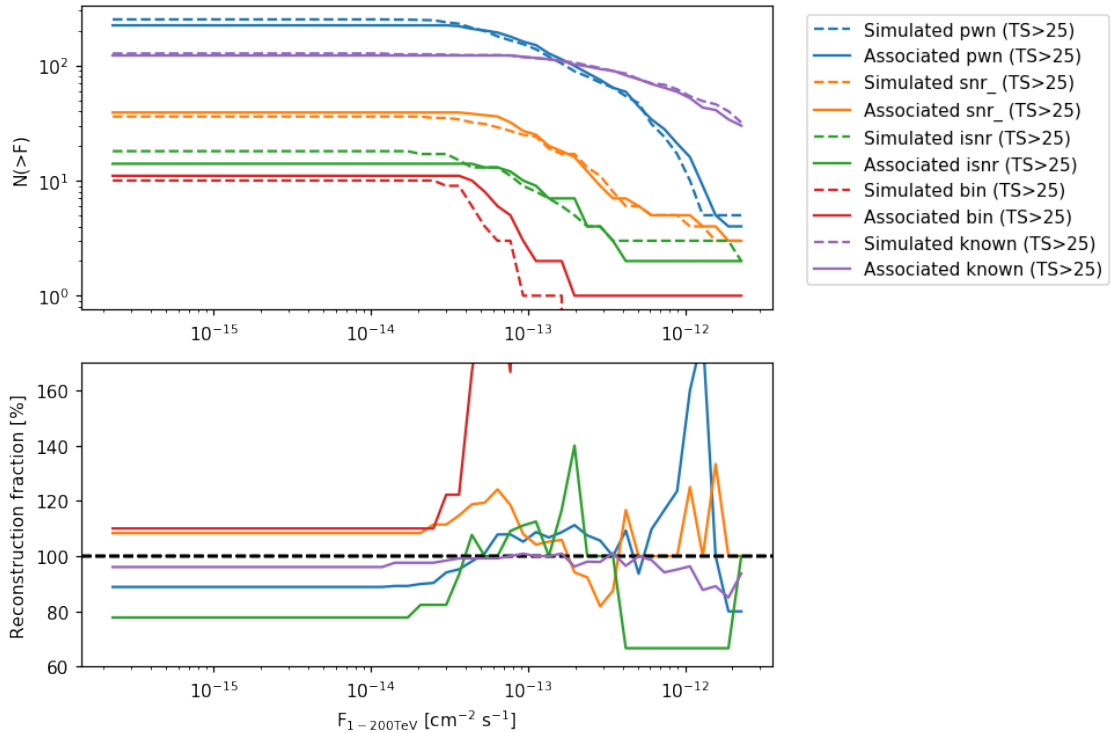
pwn simulated with TS>25 (for E = 1-200 TeV): 251
 pwn associated with TS>25 (for E = 1-200 TeV): 223

snr_ simulated with TS>25 (for E = 1-200 TeV): 36
 snr_ associated with TS>25 (for E = 1-200 TeV): 39

isnr simulated with TS>25 (for E = 1-200 TeV): 18
 isnr associated with TS>25 (for E = 1-200 TeV): 14

bin simulated with TS>25 (for E = 1-200 TeV): 10
 bin associated with TS>25 (for E = 1-200 TeV): 11

known simulated with TS>25 (for E = 1-200 TeV): 127
 known associated with TS>25 (for E = 1-200 TeV): 122

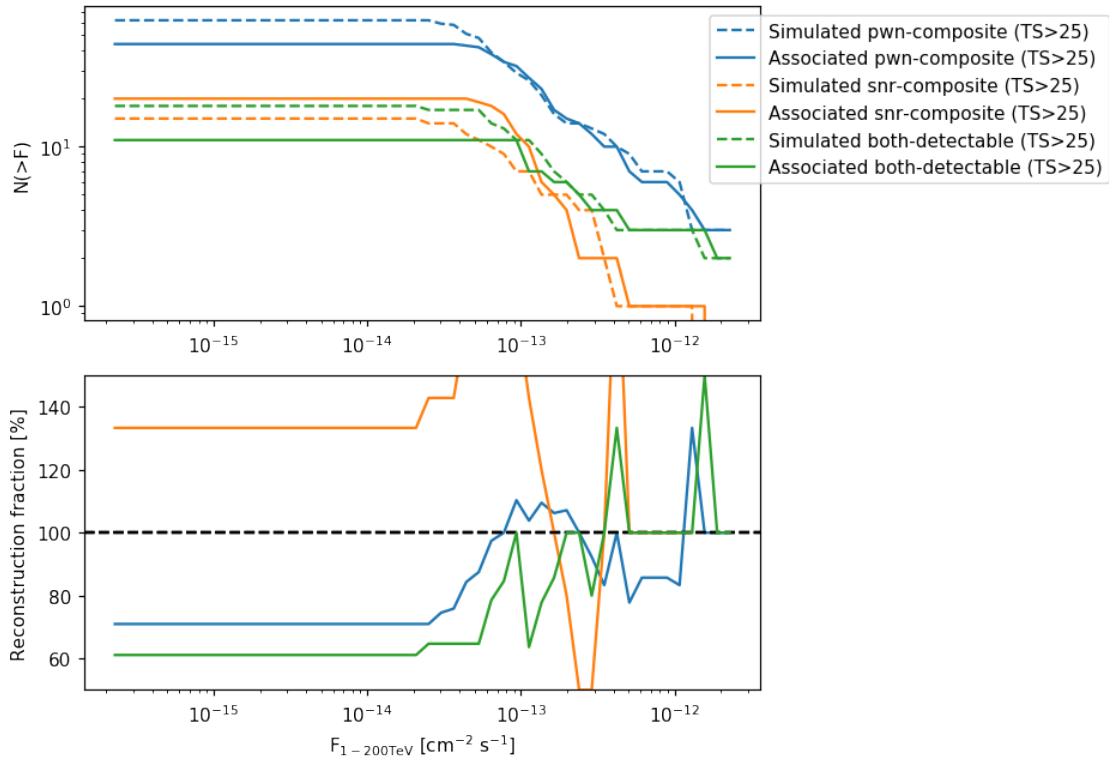


[373]: # logN-logS and reconstruction fraction composites

pwn-composite simulated with TS>25 (for E = 1-200 TeV): 62
 pwn-composite associated with TS>25 (for E = 1-200 TeV): 44

snr-composite simulated with TS>25 (for E = 1-200 TeV): 15
 snr-composite associated with TS>25 (for E = 1-200 TeV): 20

both-detectable simulated with TS>25 (for E = 1-200 TeV): 18
 both-detectable associated with TS>25 (for E = 1-200 TeV): 11



[374]: # logN-logS and reconstruction fraction per spatial model

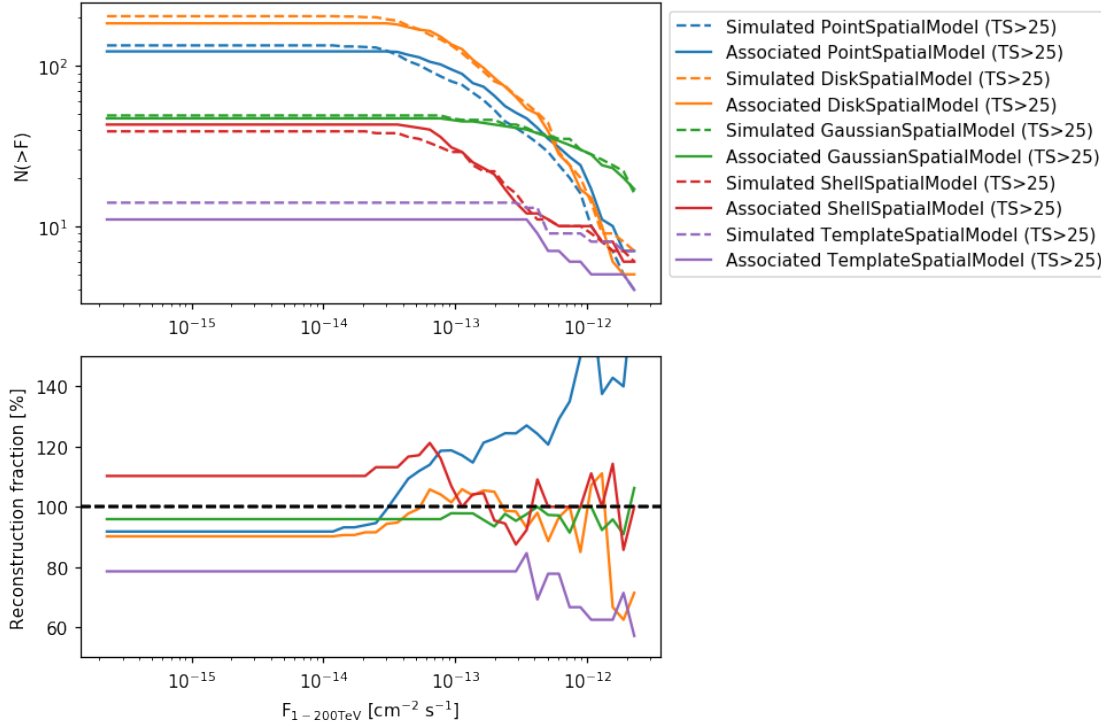
PointSpatialModel simulated with TS>25 (for E = 1-200 TeV): 134
 PointSpatialModel associated with TS>25 (for E = 1-200 TeV): 123

DiskSpatialModel simulated with TS>25 (for E = 1-200 TeV): 204
 DiskSpatialModel associated with TS>25 (for E = 1-200 TeV): 184

GaussianSpatialModel simulated with TS>25 (for E = 1-200 TeV): 49
 GaussianSpatialModel associated with TS>25 (for E = 1-200 TeV): 47

ShellSpatialModel simulated with TS>25 (for E = 1-200 TeV): 39
 ShellSpatialModel associated with TS>25 (for E = 1-200 TeV): 43

TemplateSpatialModel simulated with TS>25 (for E = 1-200 TeV): 14
 TemplateSpatialModel associated with TS>25 (for E = 1-200 TeV): 11

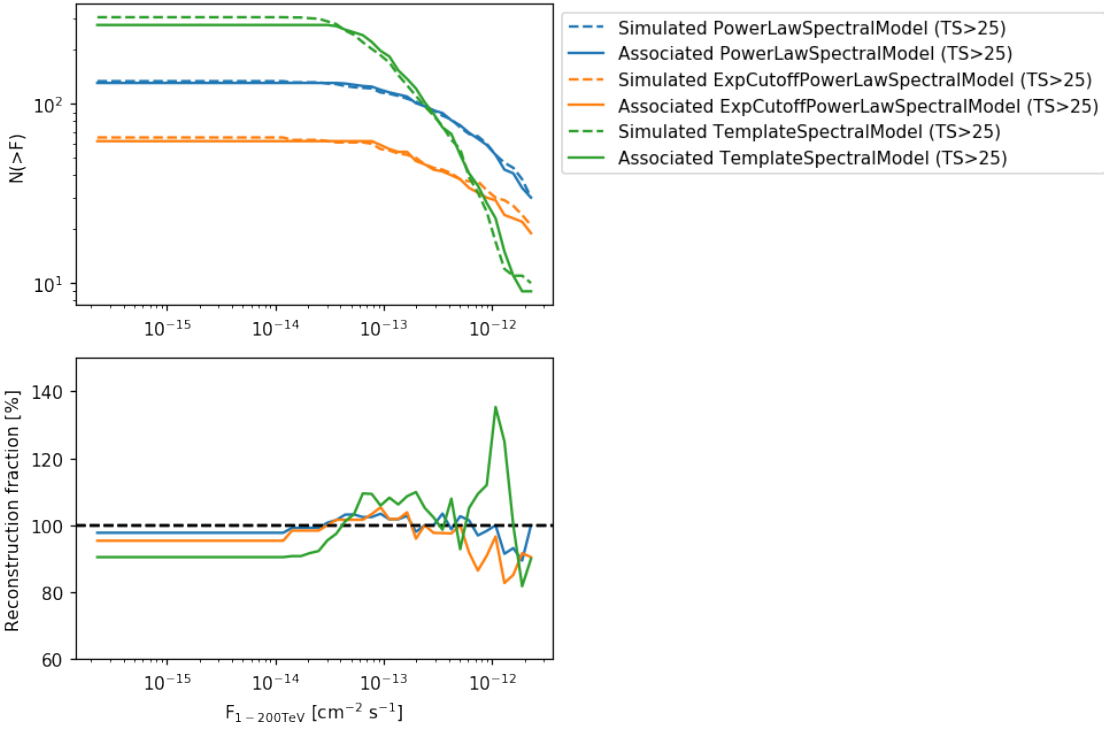


[375]: # *logN-logS and reconstruction fraction per spectral model*

PowerLawSpectralModel simulated with TS>25 (for E = 1-200 TeV): 134
 PowerLawSpectralModel associated with TS>25 (for E = 1-200 TeV): 131

ExpCutoffPowerLawSpectralModel simulated with TS>25 (for E = 1-200 TeV): 65
 ExpCutoffPowerLawSpectralModel associated with TS>25 (for E = 1-200 TeV): 62

TemplateSpectralModel simulated with TS>25 (for E = 1-200 TeV): 305
 TemplateSpectralModel associated with TS>25 (for E = 1-200 TeV): 276



4.4.5 TS: test statistic refinement

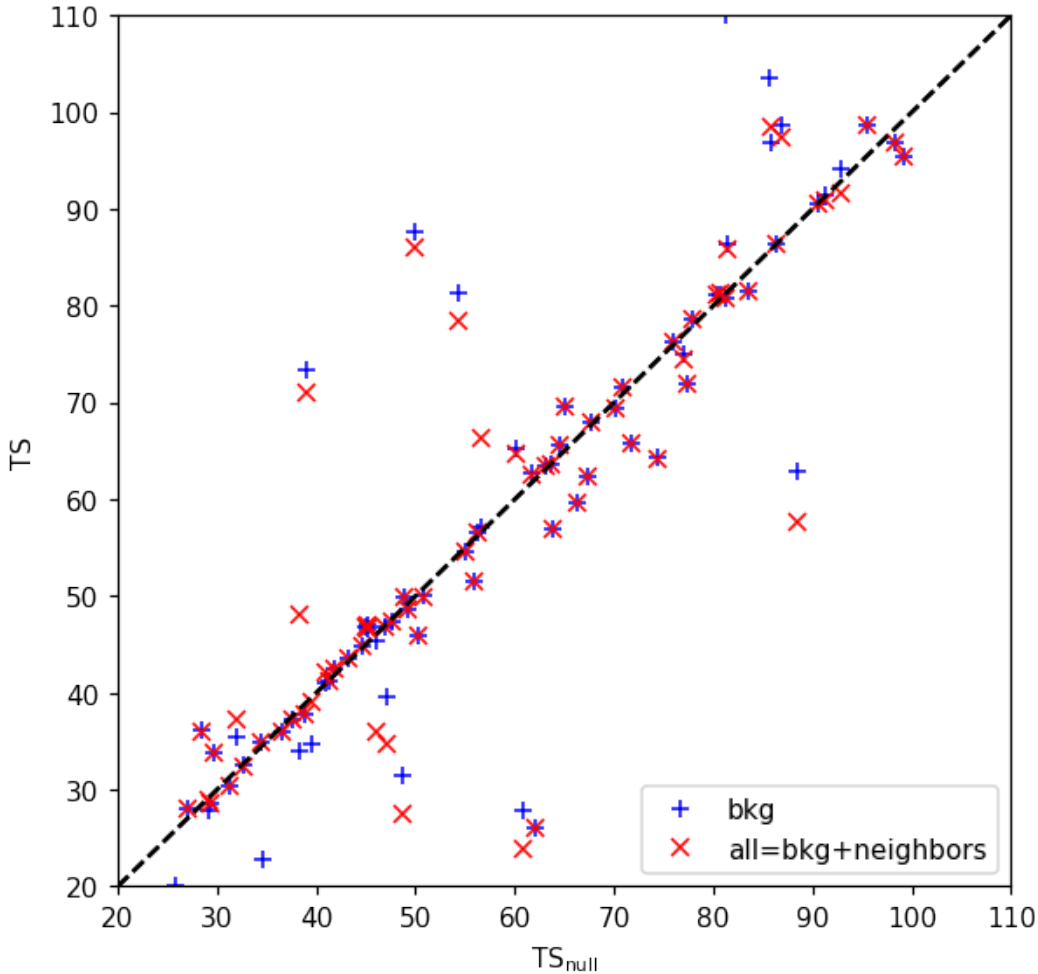
Test global model with and without each candidate source :

- TS_{null} : test against global model, all frozen (tested source amplitude frozen or zero)
- TS_{bkg} : test with background norm free (and with tested source amplitude free or zero)
- TS_{all} : test with background free + nearby sources amplitude free if $d_c < R_{\text{object}} + R_{\text{other}} + 1$ deg (and with tested source amplitude free or zero)

First compute the fastest test, TS_{null} , and discard the source with $TS_{\text{null}} < 25$ (short circuit). Then refine testing with TS_{bkg} only if $25 < TS_{\text{null}} < 100$ (above sources will very likely remain significant anyway).

Finally compute TS_{all} if $25 < TS_{\text{bkg}} < 100$. The following figure shows that only few sources present discrepancies with the refined tests so TS_{null} is quite robust and it allows comparisons with the expected TS from the exact simulated model frozen as shown in the previous plots.

[376]: # TS comparison near threshold



4.4.6 Hyper-parameter optimization : catalogue threshold

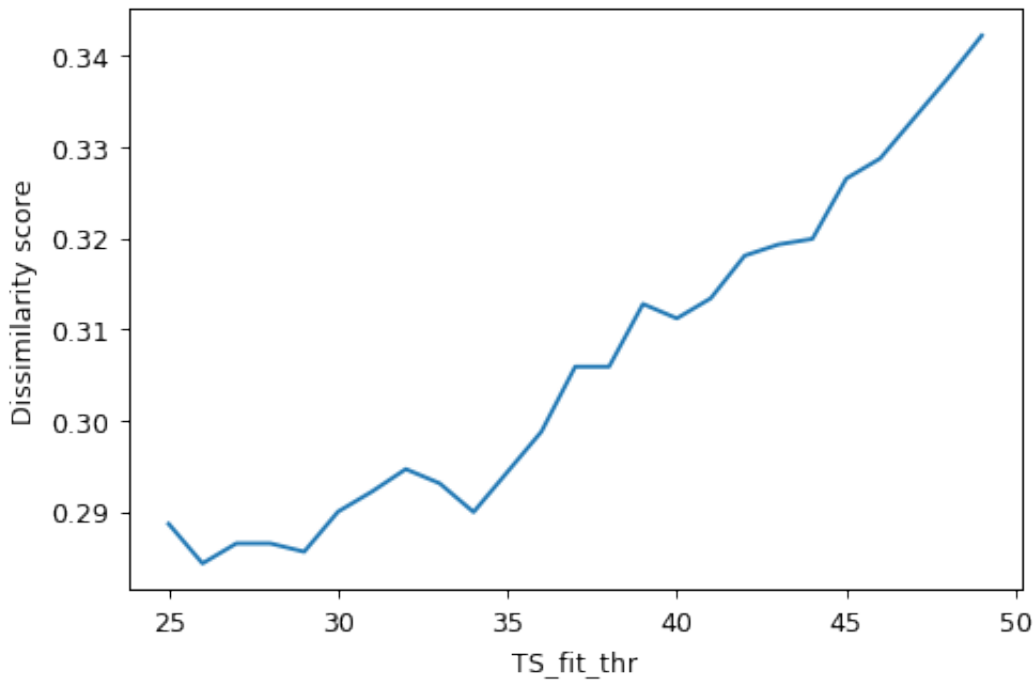
Find the TS threshold that maximize the reconstruction fraction and the association fraction (in the 1-200 TeV range). In practice the quantity minimized is the dissimilarity score that combines the information of both reconstruction and the association fractions : $d_{score} = 1 - f_{reco} \times f_{asso}$.

Note : similarly once could also optimize the minimal surface overlap criterion for associations, for now it is fixed to 25.

[377]: # Hyper-parameter optimization : catalogue threshold

```
Objects detected: 461
Objects associated (SFoverlap>0.25): 392
Reconstruction fraction (TS>10): 0.74
Reconstruction fraction (TS>30): 0.86
Association fraction: 0.85
Dissimilarity score (TS>30): 0.27
```

```
Optimal TS_fit threshold = 26 for TS_simu >= 25 with dissimilarity score = 0.28)
```



5 Post-fit classification

Filtering/merging spurious detections is more a classification problem than a statistical problem (so we need more decision criterions than only TS).

5.1 Sprecto-morphologically coherent complexes

In the following we reduce the catalogue to a list of sprecto-morphologically coherent complex by merging the sub-structures with their parent object if they do not have a different association or a different spectral shape (the optimal condition on the variance of the spectral shape could be improved by learning the typical error on alpha/beta?).

...

```
[384]: # score before merging
```

```
Score before merging
Objects detected: 526
Objects associated (SFoverlap>0.25): 434
Reconstruction fraction (TS>10): 0.77
Reconstruction fraction (TS>30): 0.88
Association fraction: 0.83
```

Dissimilarity score (TS>30): 0.27

Number of object before merging: 526

Number of complex after merging: 477

Nsource simulated with TS>25 (for E = 1-200 TeV): 442

Nsource fitted with TS>25 (for E = 1-200 TeV): 419

Nsource associated with TS>25 (for E = 1-200 TeV): 398

Score after merging

Objects detected: 477

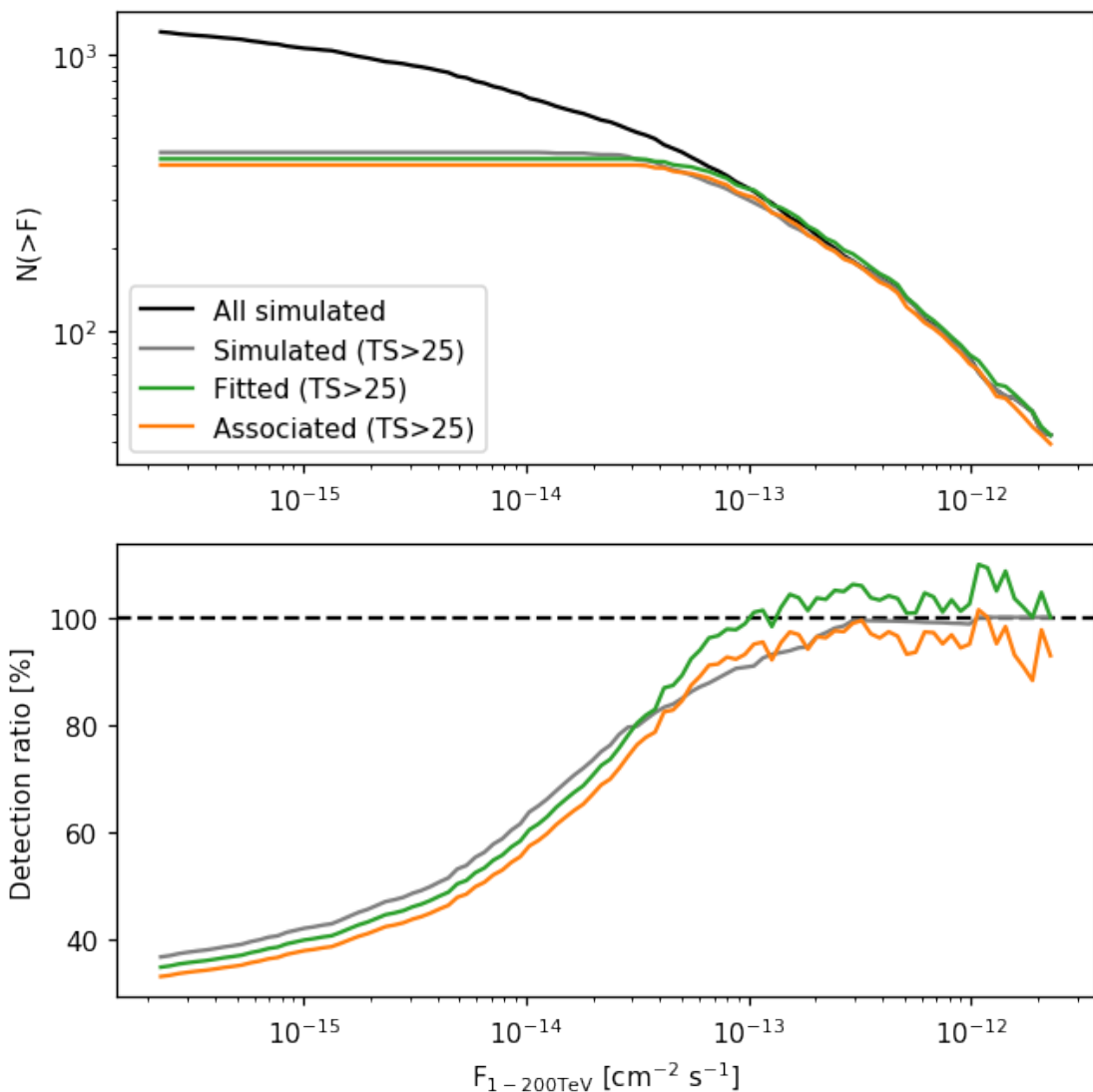
Objects associated (SFOverlap>0.25): 425

Reconstruction fraction (TS>10): 0.76

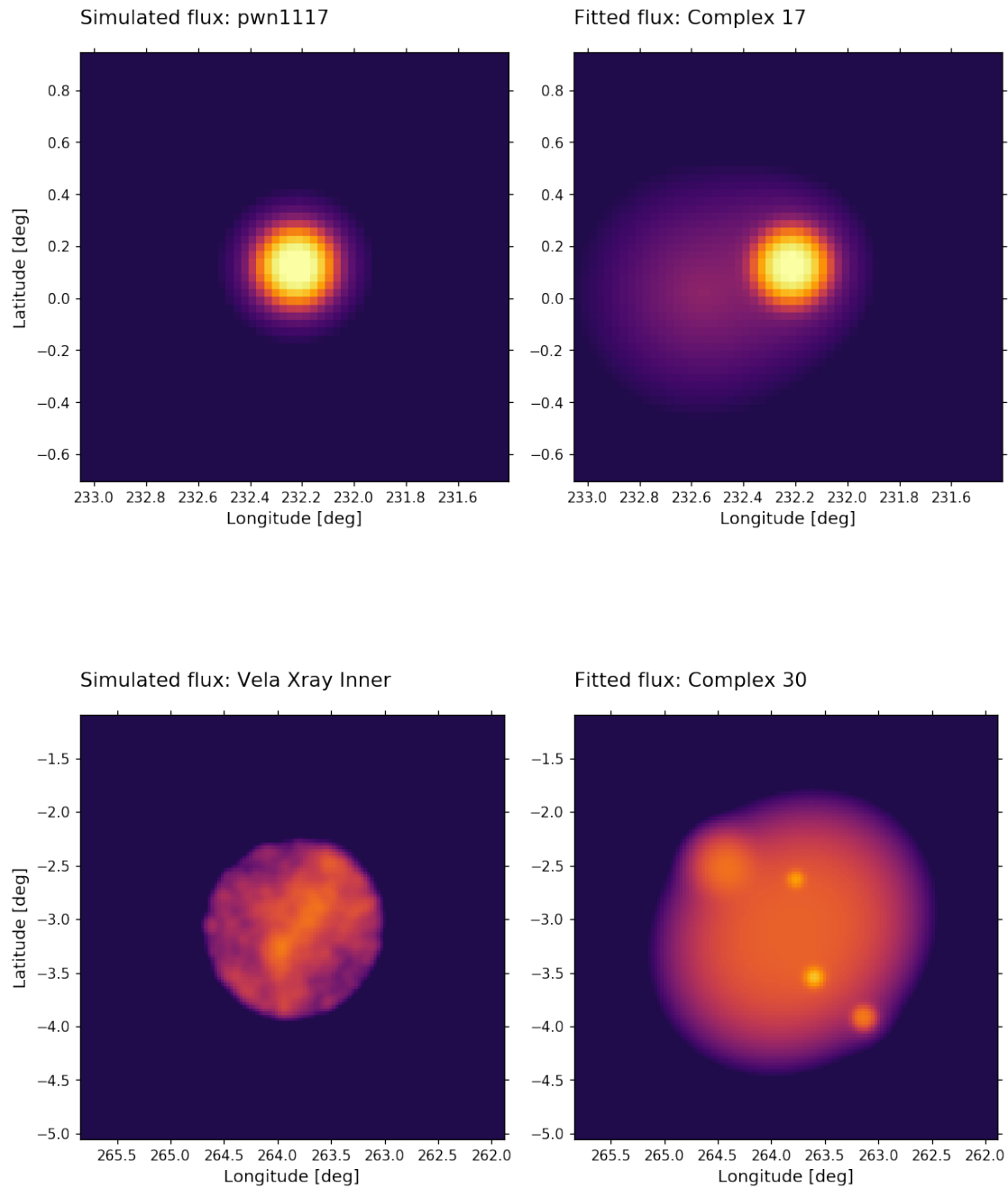
Reconstruction fraction (TS>30): 0.86

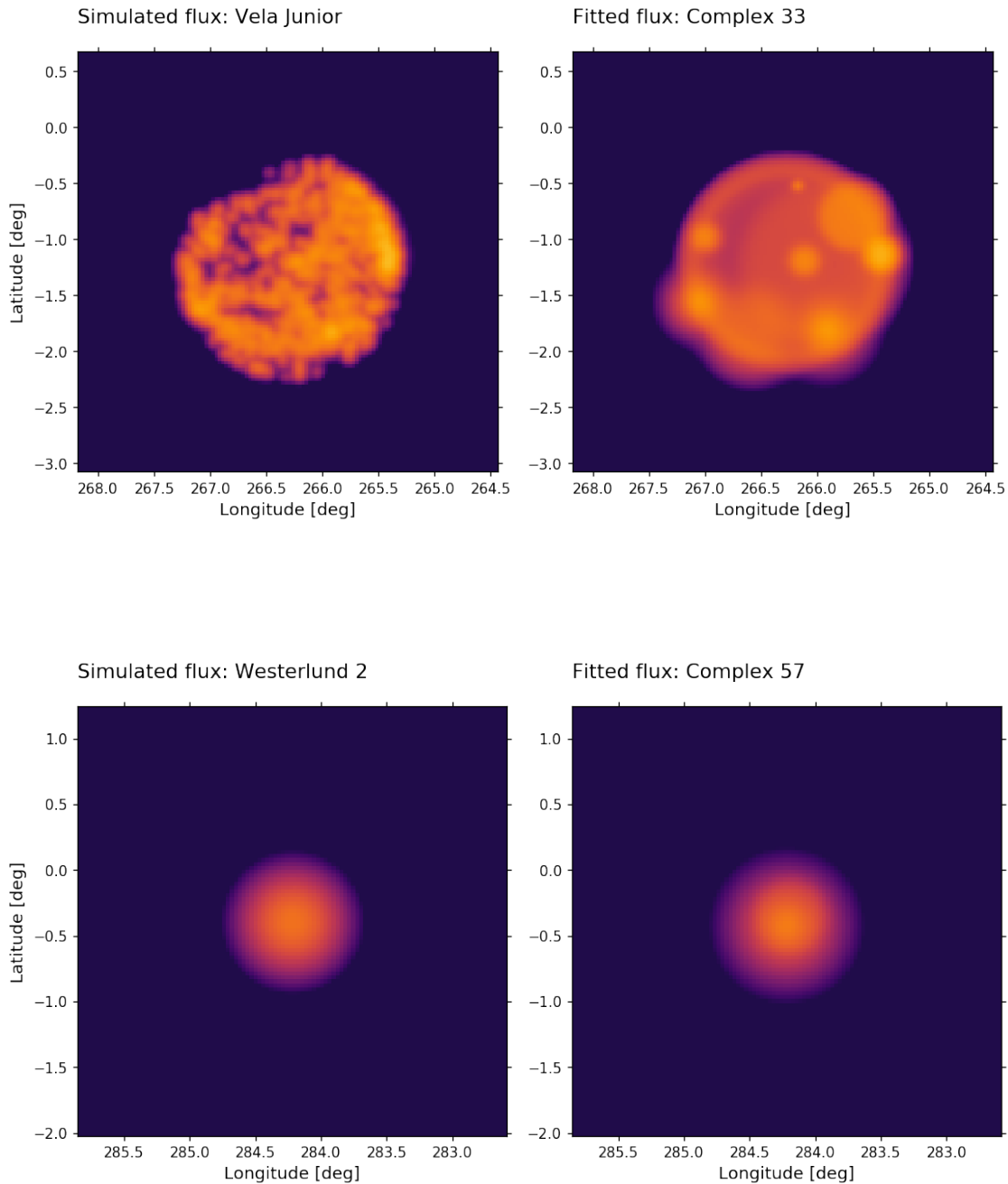
Association fraction: 0.89

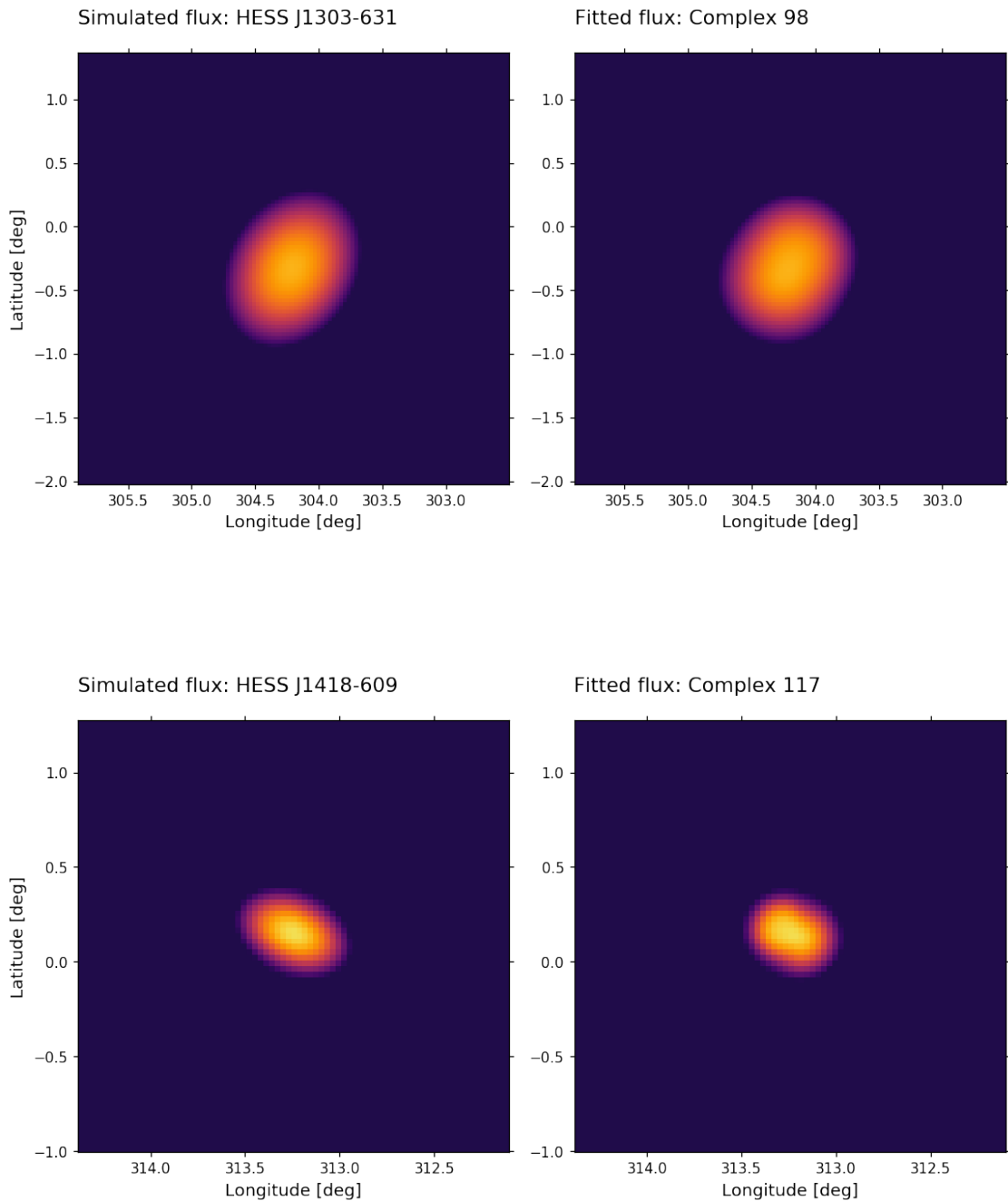
Dissimilarity score (TS>30): 0.23

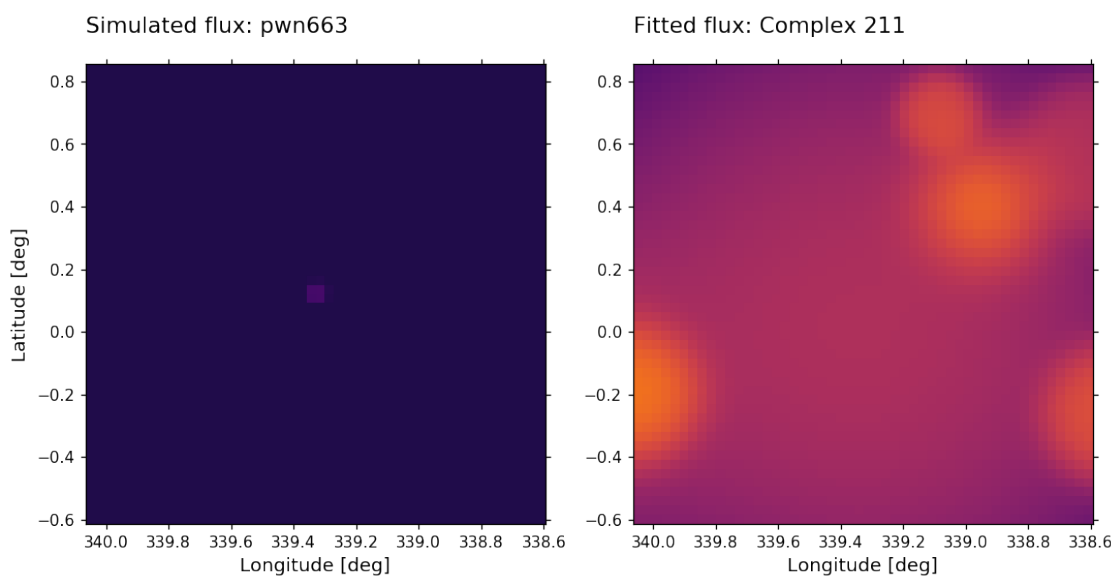
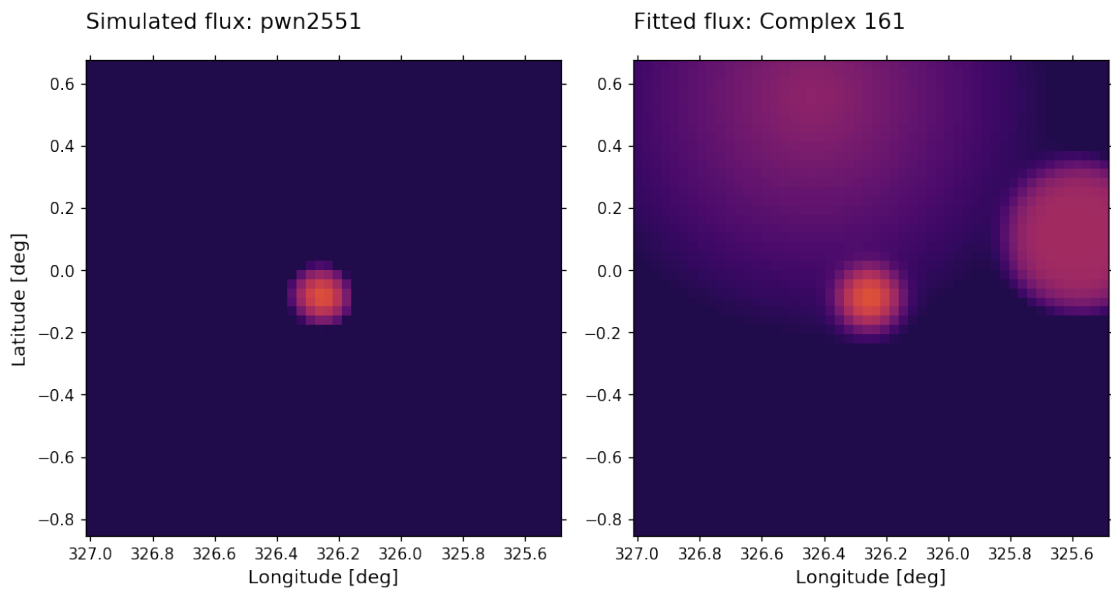


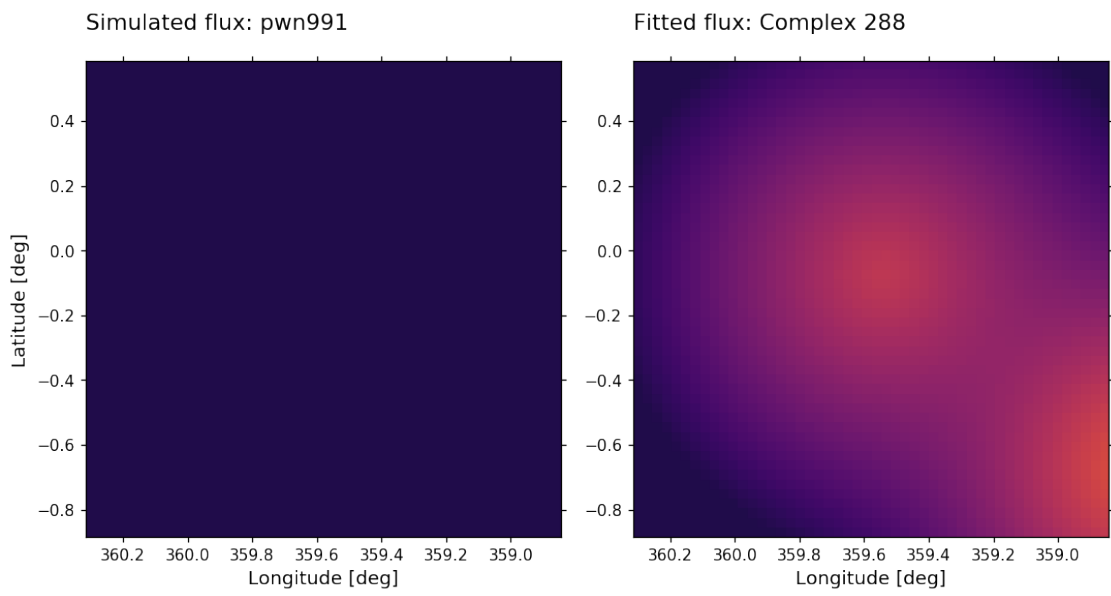
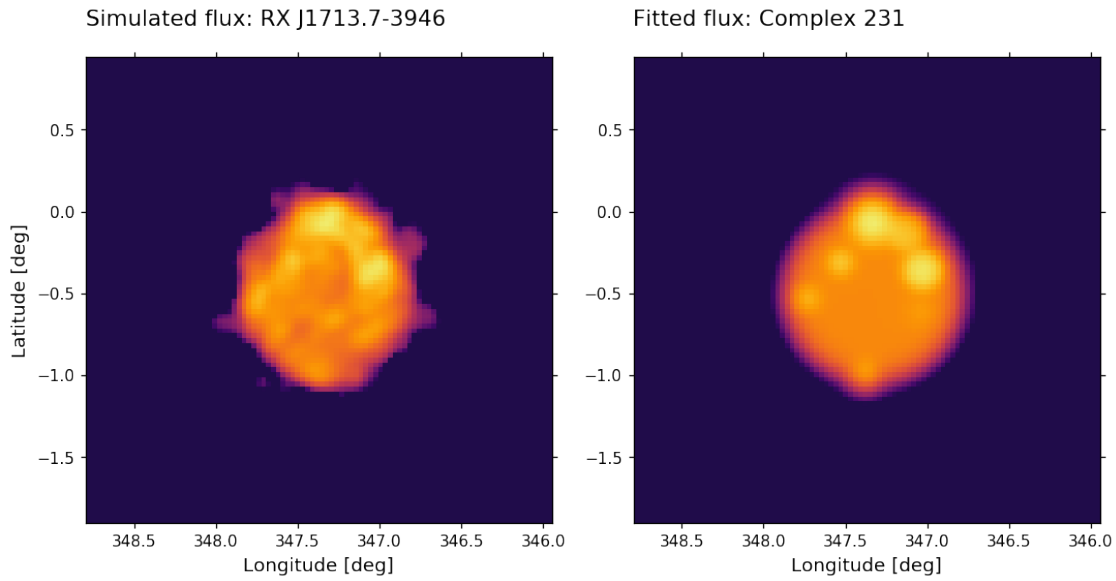
```
[387]: # Complex flux comparison with association
```

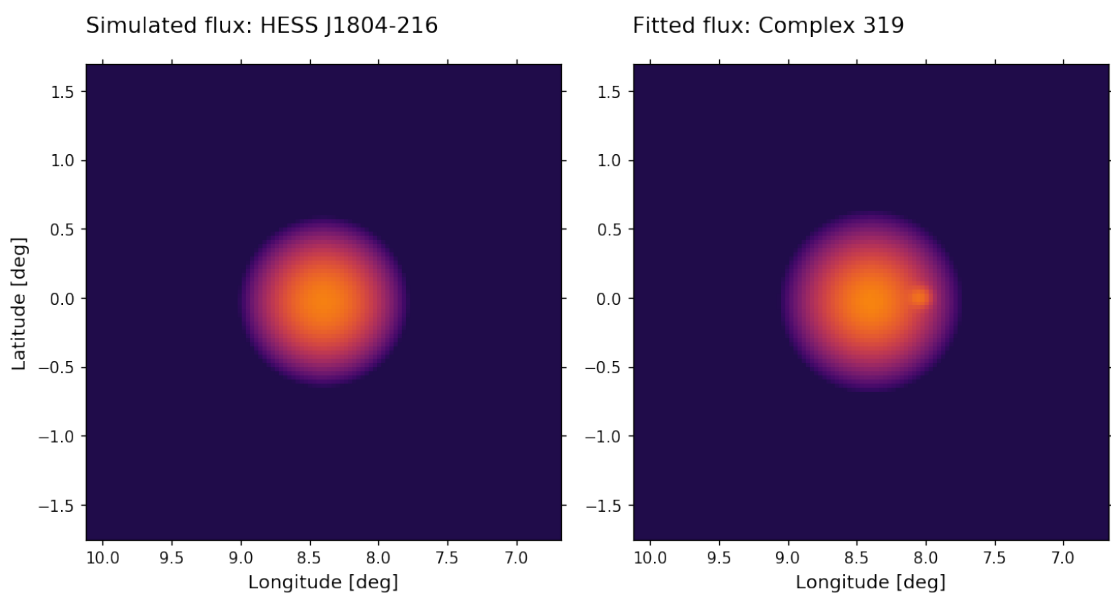
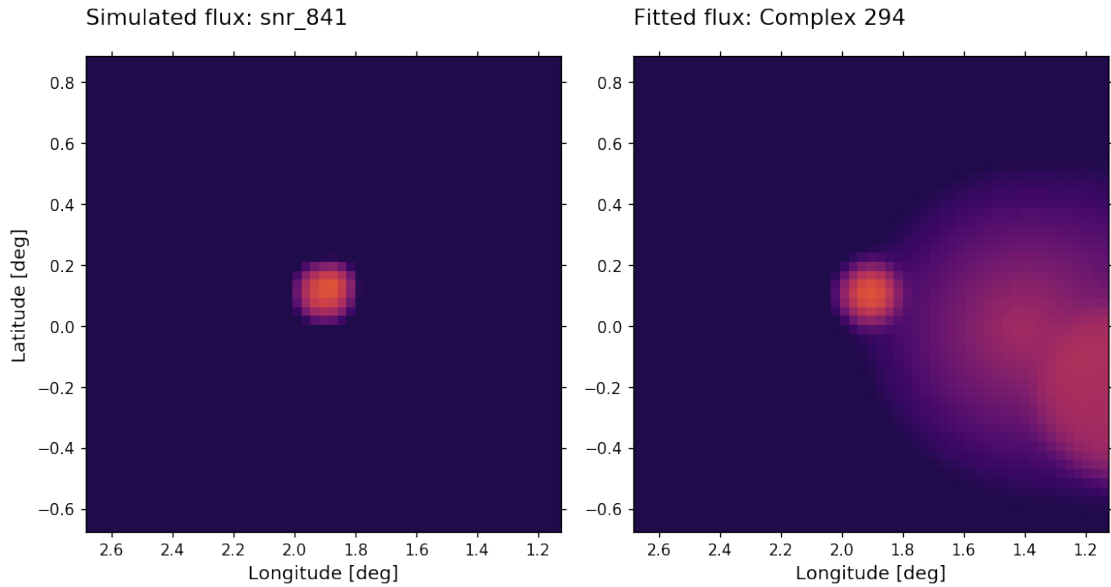


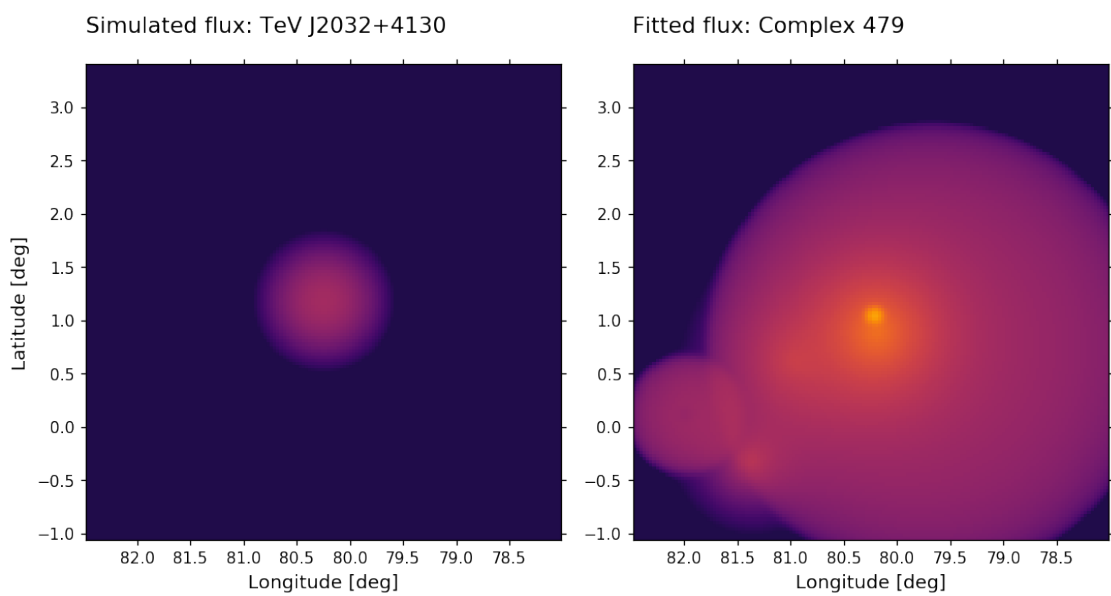
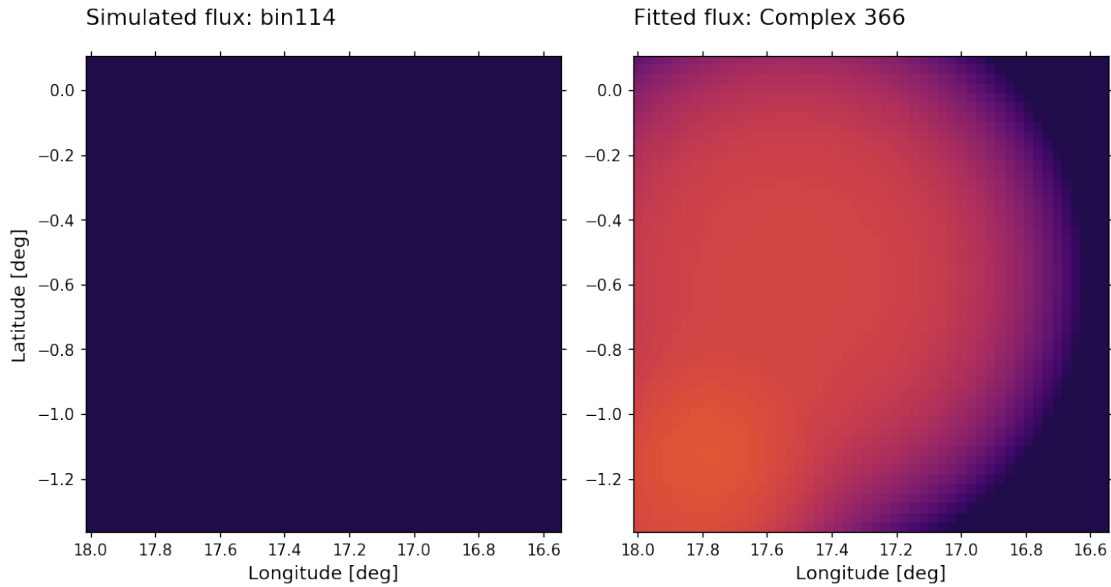


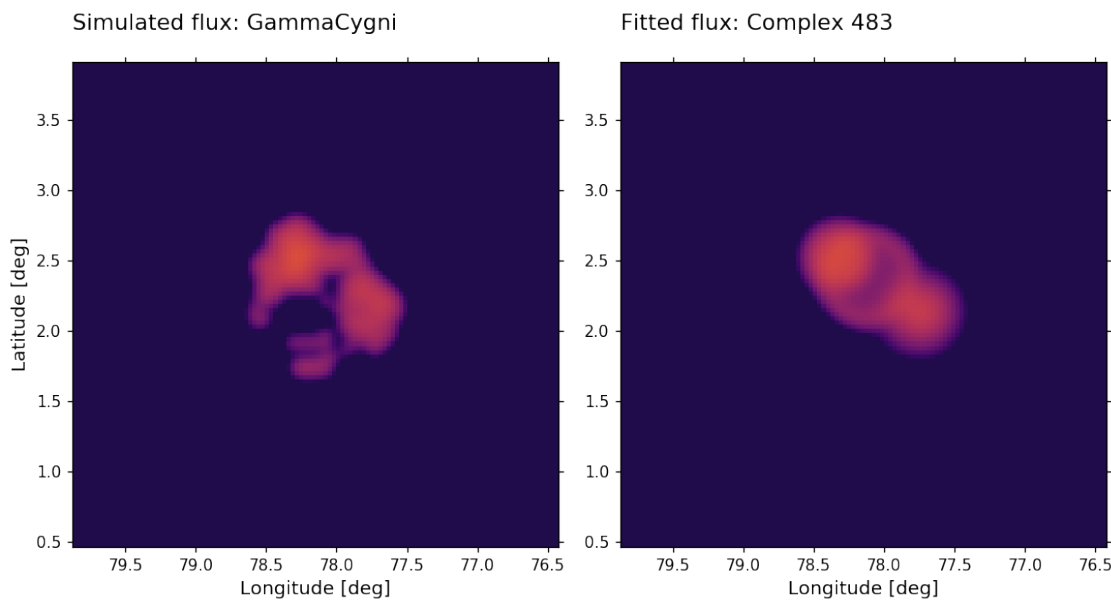












[]:

...

...